SJSU SAN JOSÉ STATE UNIVERSITY

MTI MINETA TRANSPORTATION INSTITUTE

Virus Control Aboard a Commuter Bus

Hamid Rahai, PhD
Jeremy Bonifacio, PhD

CSUTC California State University Transportation Consortium

CALIFORNIA STATE UNIVERSITY LONG BEACH

CSU TRANSPORTATION CONSORTIUM

transweb.sjsu.edu/csutc

Mineta Transportation Institute

Founded in 1991, the Mineta Transportation Institute (MTI), an organized research and training unit in partnership with the Lucas College and Graduate School of Business at San José State University (SJSU), increases mobility for all by improving the safety, efficiency, accessibility, and convenience of our nation's transportation system. Through research, education, workforce development, and technology transfer, we help create a connected world. MTI leads the Mineta Consortium for Transportation Mobility (MCTM) funded by the U.S. Department of Transportation and the California State University Transportation Consortium (CSUTC) funded by the State of California through Senate Bill 1. MTI focuses on three primary responsibilities:

Research

MTI conducts multi-disciplinary research focused on surface transportation that contributes to effective decision making. Research areas include: active transportation; planning and policy; security and counterterrorism; sustainable transportation and land use; transit and passenger rail; transportation engineering; transportation finance; transportation technology; and workforce and labor. MTI research publications undergo expert peer review to ensure the quality of the research.

Education and Workforce

To ensure the efficient movement of people and products, we must prepare a new cohort of transportation professionals who are ready to lead a more diverse, inclusive, and equitable transportation industry. To help achieve this, MTI sponsors a suite of workforce development and education opportunities. The Institute supports educational programs offered by the Lucas Graduate School of Business: a Master of Science in Transportation Management, plus graduate certificates that include High-Speed and Intercity Rail Management and Transportation Security Management. These flexible programs offer live online classes so that working transportation professionals can pursue an advanced degree regardless of their location.

Information and Technology Transfer

MTI utilizes a diverse array of dissemination methods and media to ensure research results reach those responsible for managing change. These methods include publication, seminars, workshops, websites, social media, webinars, and other technology transfer mechanisms. Additionally, MTI promotes the availability of completed research to professional organizations and works to integrate the research findings into the graduate education program. MTI's extensive collection of transportation-related publications is integrated into San José State University's world-class Martin Luther King, Jr. Library.

Report 23-21

Virus Control Aboard a Commuter Bus

Hamid Rahai, PhD

Jeremy Bonifacio, PhD

October 2023

A publication of the
Mineta Transportation Institute
Created by Congress in 1991

College of Business
San José State University
San José, CA 95192–0219

TECHNICAL REPORT DOCUMENTATION PAGE

1. Report No. 23-21	**2. Government Accession No.**	**3. Recipient's Catalog No.**	
4. Title and Subtitle Virus Control Aboard a Commuter Bus		**5. Report Date** October 2023	
		6. Performing Organization Code	
7. Authors Hamid Rahai, PhD ORCID: 0000-0003-4147-466X Jeremy Bonifacio, PhD		**8. Performing Organization Report** CA-MTI-2248	
9. Performing Organization Name and Address Mineta Transportation Institute College of Business San José State University San José, CA 95192–0219		**10. Work Unit No.**	
		11. Contract or Grant No. ZSB12017-SJAUX	
12. Sponsoring Agency Name and Address State of California SB1 2017/2018 Trustees of the California State University Sponsored Programs Administration 401 Golden Shore, 5th Floor, Long Beach, CA 90802		**13. Type of Report and Period Covered**	
		14. Sponsoring Agency Code	
15. Supplemental Notes			

16. Abstract

A major health concern for public transit users is exposure to viruses from other passengers. This numerical study examines virus containment aboard a public bus with changes to the bus ventilation system. The virus was modeled as a 2.5 μm round solid particle released from the mouth of the infectious passenger at a rate of 21 particles per second at a mouth velocity of 0.278 m/sec. The air delivery to the cabin was two linear ceiling slots spanning the length of the bus delivering 59.38 m3/min (2,097 CFM) of air at a mean velocity of 1 m/sec. Two different axial and vertical linear exhaust slots placed on the side walls were investigated to examine how they affected virus containment and spread to the other parts of the cabin. Simulations were performed for both cases of the bus in transit and at the bus stop when the drop-off door was opened. Results indicate during transit that virus spread was contained to passengers sitting immediately in front of and behind the infectious passenger and the level of virus concentration could merit an increased risk of infection with increased virus residence time. However, augmented air mixing was observed between inside and outside air during the passenger drop-off with viruses spread to the front and back of the bus with reduced concentration and risk of infection. Analytical analyses of the risk of infection using the Wells-Riley equation were performed for the bus ventilation using 100% recirculating air without filtration, and 50% and 100% fresh air ventilation. Results indicate a high risk of infection when recirculating air is used, but the risk is reduced significantly with 50% and 100% fresh air ventilation. These results are critical to informing bus manufacturers, transit agencies, planners, and public transportation users about the potential of virus containment using a new ventilation system.

17. Key Words Virus Transport, Passengers' Health, Indoor Air Quality, Vehicle's HVAC System, Numerical Simulation	**18. Distribution Statement** No restrictions. This document is available to the public through The National Technical Information Service, Springfield, VA 22161.		
19. Security Classif. (of this report) Unclassified	**20. Security Classif. (of this page)** Unclassified	**21. No. of Pages** 59	**22. Price**

Form DOT F 1700.7 (8–72)

DOI: 10.31979/mti.2023.2248

Mineta Transportation Institute
College of Business
San José State University
San José, CA 95192–0219

Tel: (408) 924–7560
Fax: (408) 924–7565
Email: mineta-institute@sjsu.edu

transweb.sjsu.edu/research/2248

Acknowledgments

Funding for this research was provided by the State of California SB1 2022 through the Trustees of the California State University (Agreement #) and the California State University Transportation Consortium. The authors thank Editing Press for editorial services, as well as MTI staff.

CONTENTS

LIST OF FIGURES

Executive Summary

A major health concern for the population riding on public transportation systems is exposure to viruses released by infectious passengers. Our previous transient investigations[17] of virus transport from an infectious passenger sitting in the middle of a transit bus with air exiting through the back grille has shown that while viruses spread to the back and front of the bus, due to the level of their concentration, there is an increased risk of infection to passengers sitting adjacent and behind the infectious person during transit when the passenger drop-off door is closed. However, at the bus stop when the drop-off door is opened, the exposure risk was for passengers sitting in front of the infectious person. The study exemplified the importance of the bus ventilation system on the exposure risk aboard a transit bus.

The present investigation is a continuation of our previous study with changes to the bus ventilation system with the goal of virus containment. Unsteady numerical simulations of virus spread aboard a transit bus with 37 passengers have been performed. The infectious passenger was sitting in an aisle seat in the middle of the bus releasing 1267 viruses per minute (21.2 particles per second). The mouth velocity was 0.278 m/s (0.3 CFM). The virus was modeled as a 2.5 μm round carbon particle. Fresh air was injected through two linear ceiling slots spanning the length of the bus at a speed of 1 m/s The volume flow rate was 59.38 m3/min (2097 CFM). The bus dimensions were taken from a standard transit bus used in Long Beach, California.

Two linear axial and vertical exhaust slots have been investigated. The axial slots were placed 20.32 cm above the floor with a width of 5.08 cm. There were two slots on each side of the bus covering the length of the bus adjacent to the seats. The vertical slots were placed between the windows, 66.04 cm above the floor. The slot length and width were respectively 30.48 and 5.08 cm. There were five slots on the left-hand side and seven slots on the right-hand side of the bus. The right-hand side includes the passenger drop-off door. The pressure at the slots was -35 Pa. For each case, simulations were performed with a closed door during transit conditions and with an open door at bus stops.

For the axial slot, results for transit conditions show particles are contained to the adjacent and immediate front and back of the infectious passenger without spreading to the back of the bus or across the aisle. The particles' concentration in these areas is related to the local mean velocity gradient and vorticity distribution. At the bus stop, when the drop-off door is opened, particles disperse further to the front of the bus but stay on the same side. After the door is closed, some particles move toward the rear of the infectious passenger, but the majority of the particles are concentrated in the front three rows of the infectious passenger.

With the vertical slots, during transit, the particles' dispersion is limited, and the majority of the particles are concentrated around the infectious person. When the drop-off door is opened,

particles move toward the entire back of the bus, indicating a higher rate of mixing in this condition.

An analytical analysis using the Wells-Riley equation indicated a high risk of infection when the ventilation is off and a reduced risk of infection for both cases investigated.

1. Introduction

The spread of a virus from infected passengers, and the release and spread of contaminants aboard public transportation systems are major public health and homeland security concerns. Since the onset of the COVID-19 pandemic, significant research and scholarly publications have been presented on virus characterization, spread, and masking. These scientific findings have been presented in a database by the world health organization (WHO) [1].

The risk of acquiring a virus within an environment depends on the virus's infectious particle concentration in the air and the immune status of the exposed individuals. In addition to its concentration, virus transport also depends on ambient temperature and humidity, and the level of air recirculation. Coughing, sneezing, talking, and breathing generates a cloud of airborne particles with diameters between a few millimeters to less than 1 μm [2–6]. While large and medium-sized droplets settle on the floor within a few minutes, those with sizes less than 10 μm are airborne for a long time and circulate through the ventilation system [7, 8]. Thus, fine particle aerosols play a role in the transmission of the virus. Temperatures above 70 ˚C destroy infectivity in a few seconds [9]. Low temperature and humidity facilitate the transmission of the virus while the transmission process becomes less efficient when the temperature and humidity are above 30 ˚C and 50%, respectively [10–12].

A recent clinical study [13] focused on the effectiveness of surgical masks on the spreading of the Coronavirus, the Influenza virus, and the Rhinovirus in the exhaled breath and cough of children and adults with acute respiratory illness. Among the 246 participants, 50% were randomly assigned to wear masks, and the rest were without masks. The exhaled breath of the participants was measured for virus detection in a real-life situation. Those with the Coronavirus or/and Influenza and not wearing masks did not shed detectable virus in their droplets and aerosols. However, the results were the opposite in participants with the Rhinovirus which was detected in 54% of the participants' aerosols. These findings also indicate that surgical masks can effectively reduce the transmission of Influenza virus particles into the environment in respiratory droplets, but not in aerosols.

Previous investigations [14–16] on virus transport aboard a commercial plane have shown that an infectious person can expose passengers in the front and adjacent seats from them, and those sitting adjacent to windows have a higher risk of exposure due to an increased virus residence time. Distancing (vacating middle seats) and/or masking significantly reduce the risk of infection to the other passengers.

For a commuter bus with an infected passenger sitting in an aisle seat in the middle of the bus, transient simulations of virus transport have shown a high risk of exposure to passengers sitting adjacent and immediately behind the infectious person when air exchange occurs at the bus stop [17]. However, the risk of infection was low for a 30-minute exposure during bus transit.

The present investigation is a continuation of our previous investigation [17] with changes in the ventilation system, allowing air exhaust channels on the side walls of the bus. Two cases of vertical line exhaust between the windows and linear axial exhaust near the passenger's foot have been investigated to reduce virus transmission and exposure risk to other passengers. To the authors' knowledge, the proposed changes to the ventilation system have not been implanted in any new transit buses.

2. Numerical Investigations

2.1 Numerical Model

The same commuter bus model as in our previous investigation [17] was used. Figure 1a shows the model. The bus had 37 seats and was fully occupied. Its dimensions were 12.82 m in length, 2.4 m in width, and 2.58 m in height. Two linear slots in the ceiling delivered air inside. The airflow was uniform at 1 m/sec with a total volume flow rate of 59.38 m^3/min (2097 CFM).

Instead of having the inside air exiting through the back grille, two separate cases of axial and vertical linear slots have been investigated. Figure 1b shows the two configurations. For the axial slot, the distance between the floor to the center of the slot was 20.32 cm with a width of 5.08 cm. There were two slots on each side of the bus, and they ran the total length of the corresponding section of the bus. The vertical slots were placed between the windows at 66.04 cm from the floor. The length and width of the slots were 30.48 cm and 5.08 cm, respectively. There were five slots on the left side and seven slots on the right side of the bus.

The infectious passenger was sitting in an aisle seat (Figure 1c). The passenger continuously released 2.5 μm round carbon particles at a rate of 21.1 particles/s. The particles simulate an aerosolized virus without evaporation. The mouth velocity was 0.278 m/s which corresponds to a volume flow rate of 0.0084 m^3/min (0.3 CFM). A non-stick boundary condition was used for the particles.

Figure 1. (a) The Numerical Model (b) Axial and Vertical Linear Slots (c) The Infectious Passenger

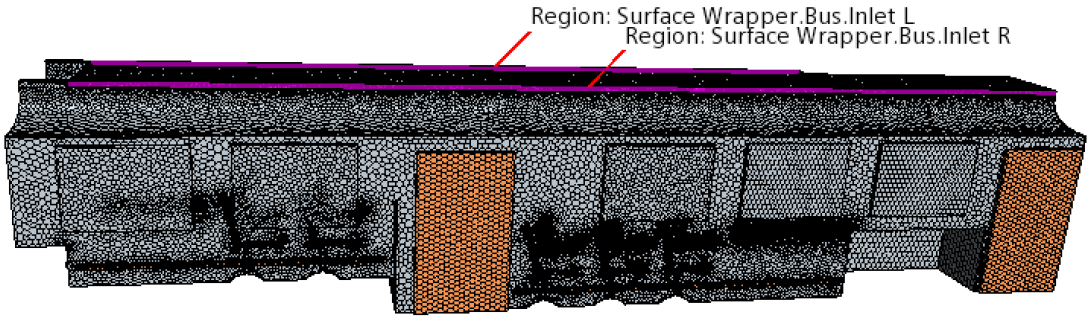

(a)

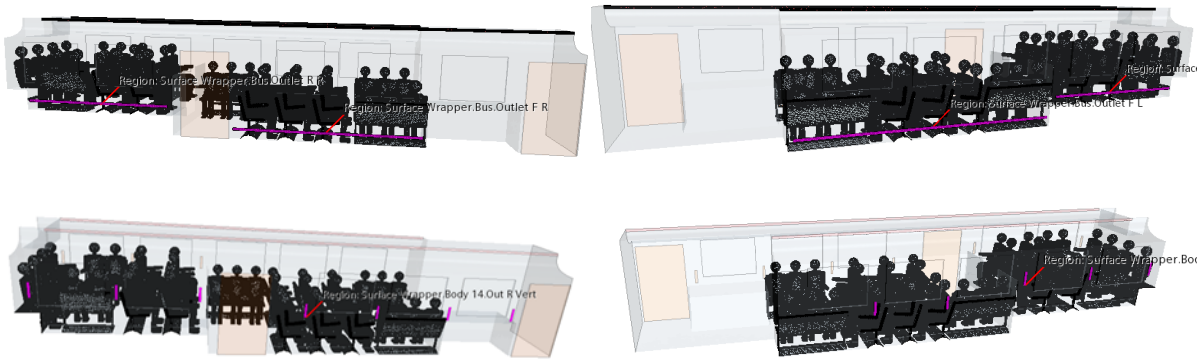

(b)

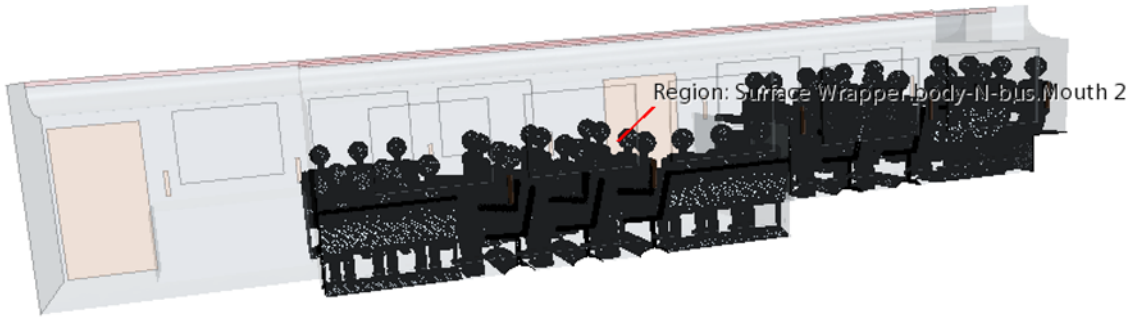

(c)

2.2 Numerical Simulations

Three-dimensional unsteady Reynolds-Averaged Navier Stokes (U-RANS) simulations were performed using the Siemens CCM+ software with an SST k-ω turbulence model. The particle simulation was modeled using a Lagrangian multiphase method. A Polyhedral mesh was used for all simulations. The number of meshes for the cases with axial and vertical slots was, respectively, 12 million and 12.1 million. The pressure boundary condition at the slots was -35 Pa. All simulations were performed on 64-core high-performance computing. As before, the simulations were performed with the passenger drop-off door being closed for 5 minutes and then opened for 30 seconds. This process was repeated several times to determine the flow characteristics inside the bus.

In addition to the axial mid-section plane, results are also presented for three monitoring vertical planes, as identified in Figure 2. These planes correspond to areas near the infectious passenger and the drop-off door where significant variations in air movements and virus concentration were expected.

Figure 2. The Monitoring Planes

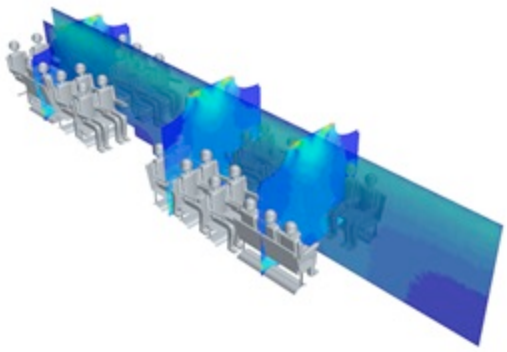

3. Results and Discussions

3.1 The Axial Exhaust Slots

Figures 3–5 show the contours of the mean velocity and pressure, and particles' dispersion at 30s intervals with axial exhaust slots when the drop-off door is closed. Figures 6 and 7 show the corresponding results for axial vorticity and turbulence kinetic energy (TKE). The presence of the axial slots on both sides of the bus increases the air circulation around the seated passengers. The mean velocity contours for the axial mid-section plane are not as uniform as before, as the axial slots extract more air toward the seated passengers and windows. The variations of the mean pressure are opposite to the corresponding variations for the mean velocity where low pressure corresponds to increased velocity and vice-versa.

When the particles are released at 30 s, they initially disperse to the front-row passengers before spreading to the rear rows. However, the dispersion and the particle concentration are limited to the front and rear rows of the infectious passenger with no dispersion to the back of the bus. These results indicate that the linear exhaust slots are successful in containing the particles' dispersion and in limiting their concentration to a small area around the source.

Because of the additional air volume around the passengers, vorticity is not uniform at the mid-section plane, and the increased vorticity around the seated passengers is due to the increase in velocity gradients within the vertical monitoring planes.

The contours of turbulence kinetic energy (TKE) show an increase around the seated passengers when the passengers are facing each other. This could be explained by the fact that for the seated passengers in rows, the obstruction and blockage caused by the passengers limits turbulence generation, and thus TKE is not increased around the passengers seated in rows. However, obstruction and blockage are reduced for passengers facing each other, leading to higher air movement and increased turbulence.

Figure 3. Contours of the Mean Velocity with a Closed Door

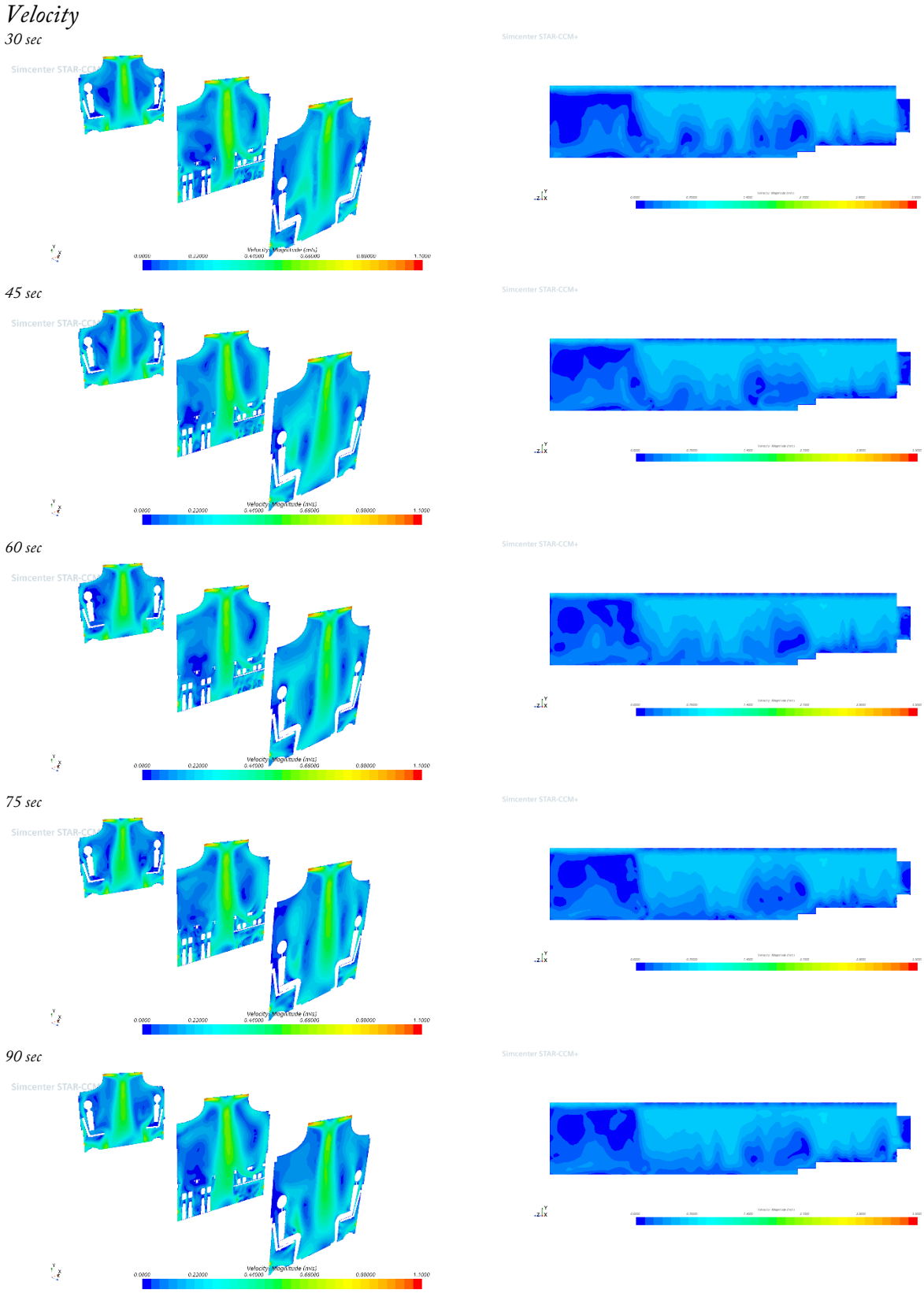

Figure 4. Contours of Mean Pressure with a Closed Door

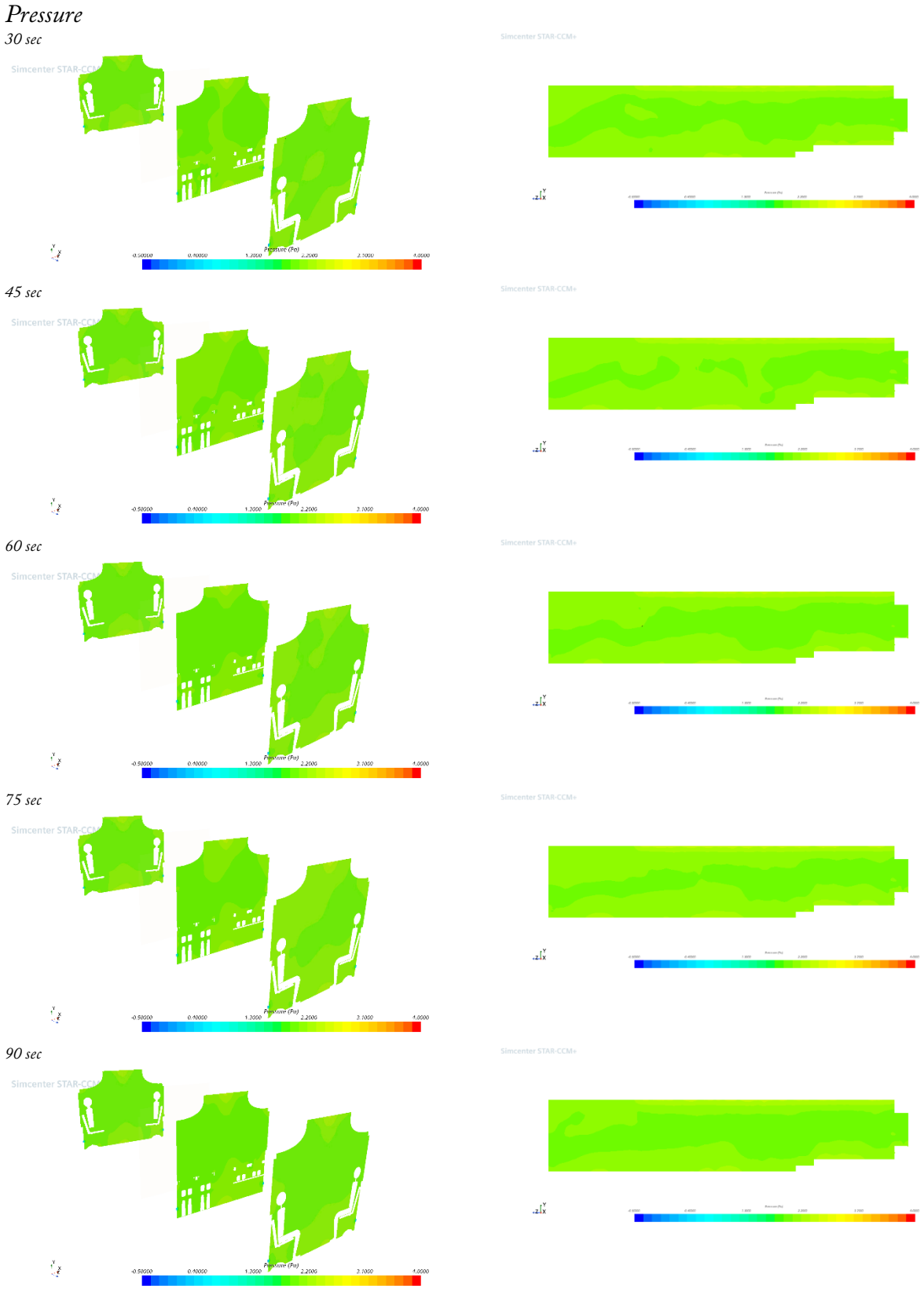

Figure 5. Particles' Dispersion with a Closed Door

Particles

30 sec

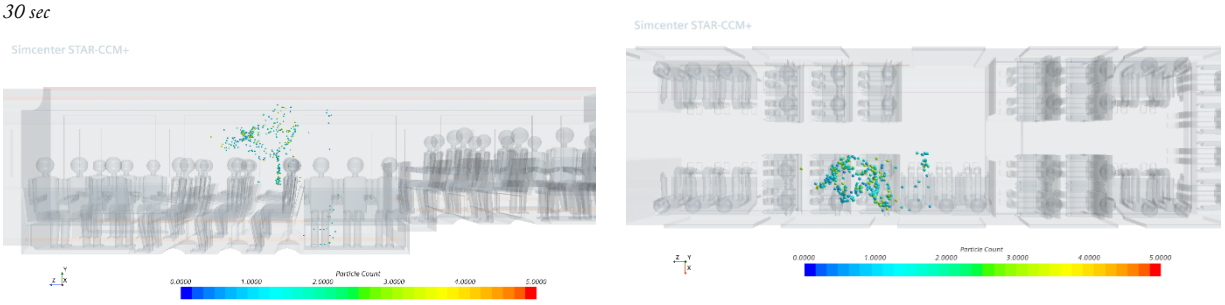

45 sec

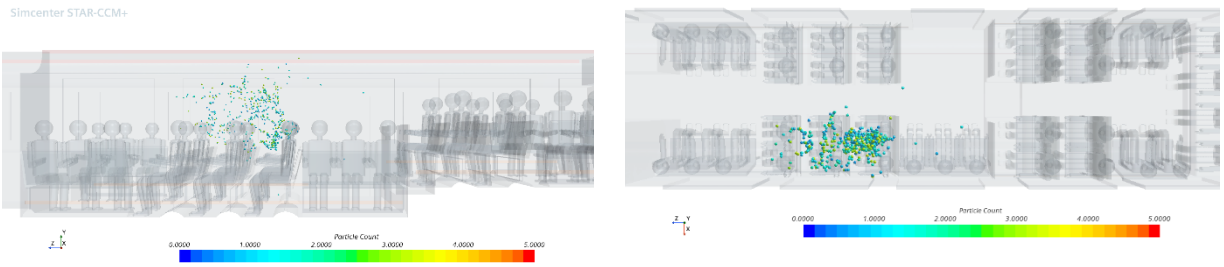

60 sec

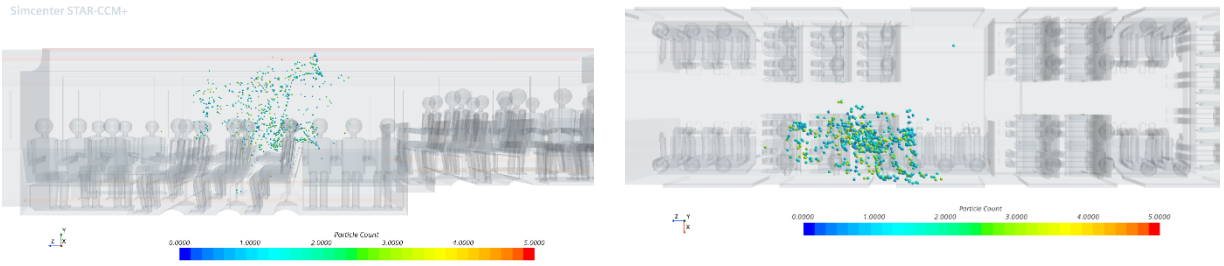

75 sec

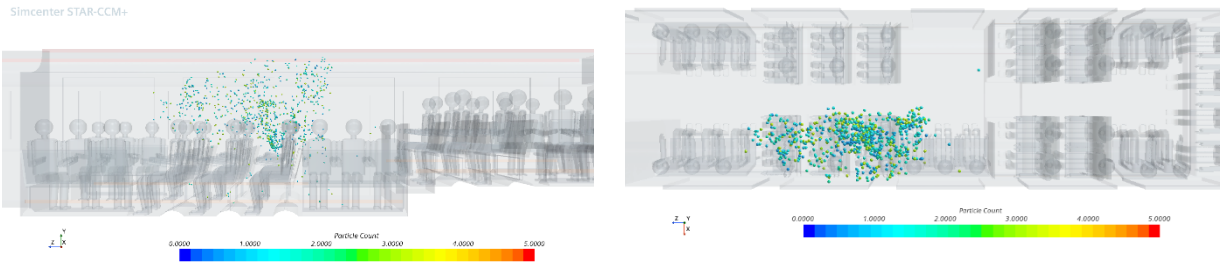

90 sec

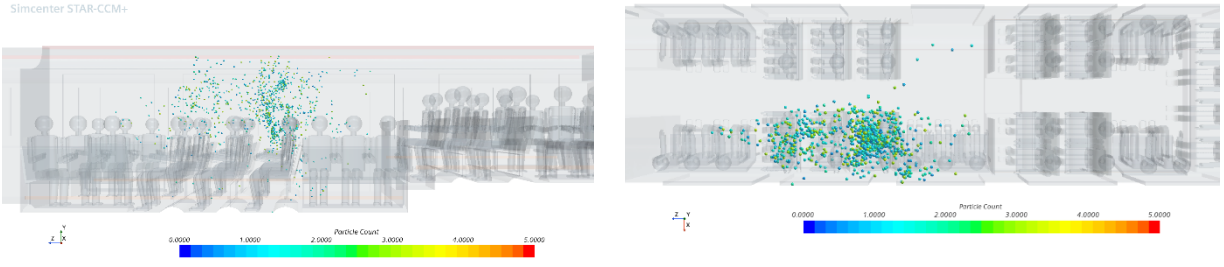

Figure 6. Contours of Axial Vorticity with a Closed Door

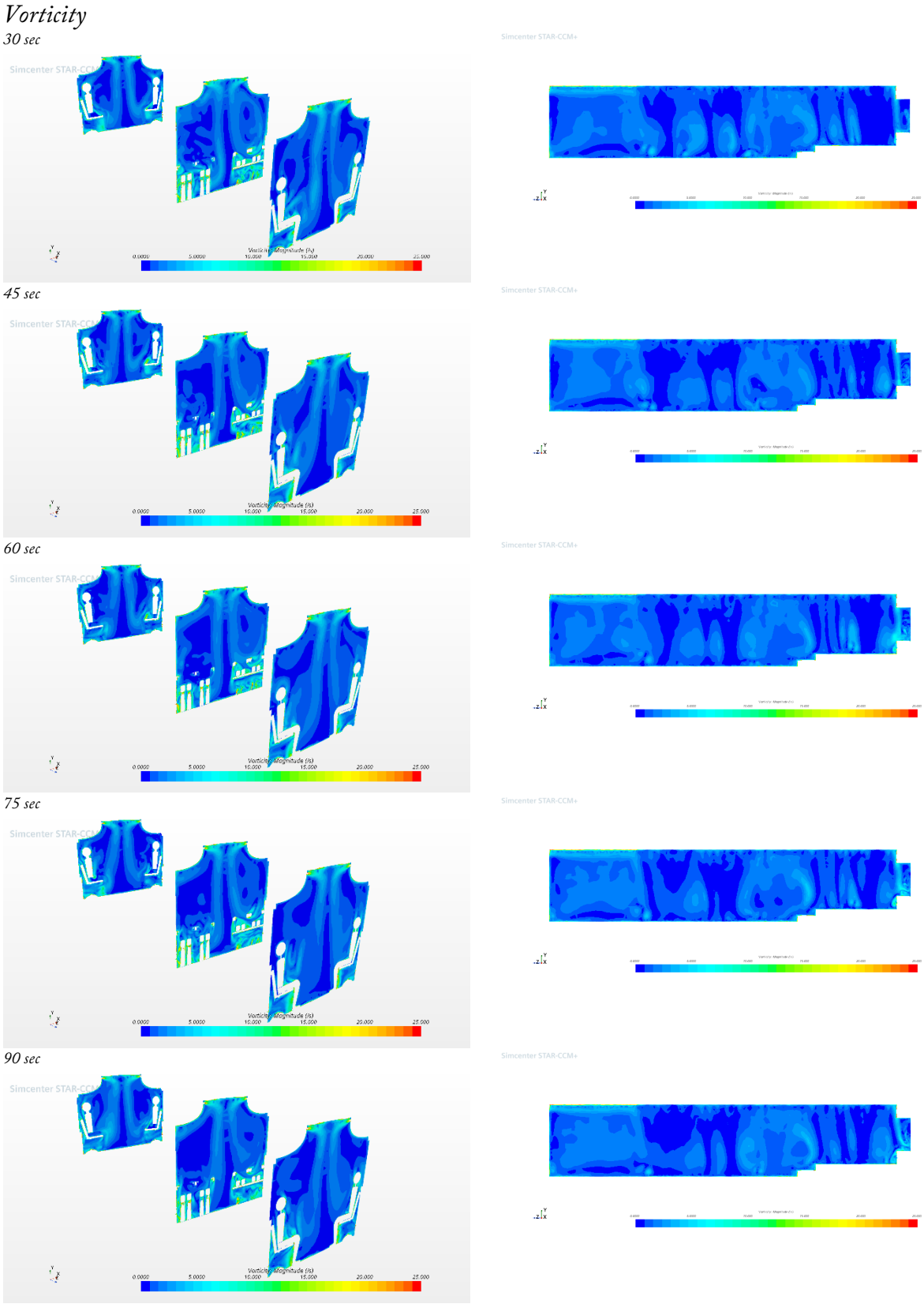

Figure 7. Contours of TKE with a Closed Door

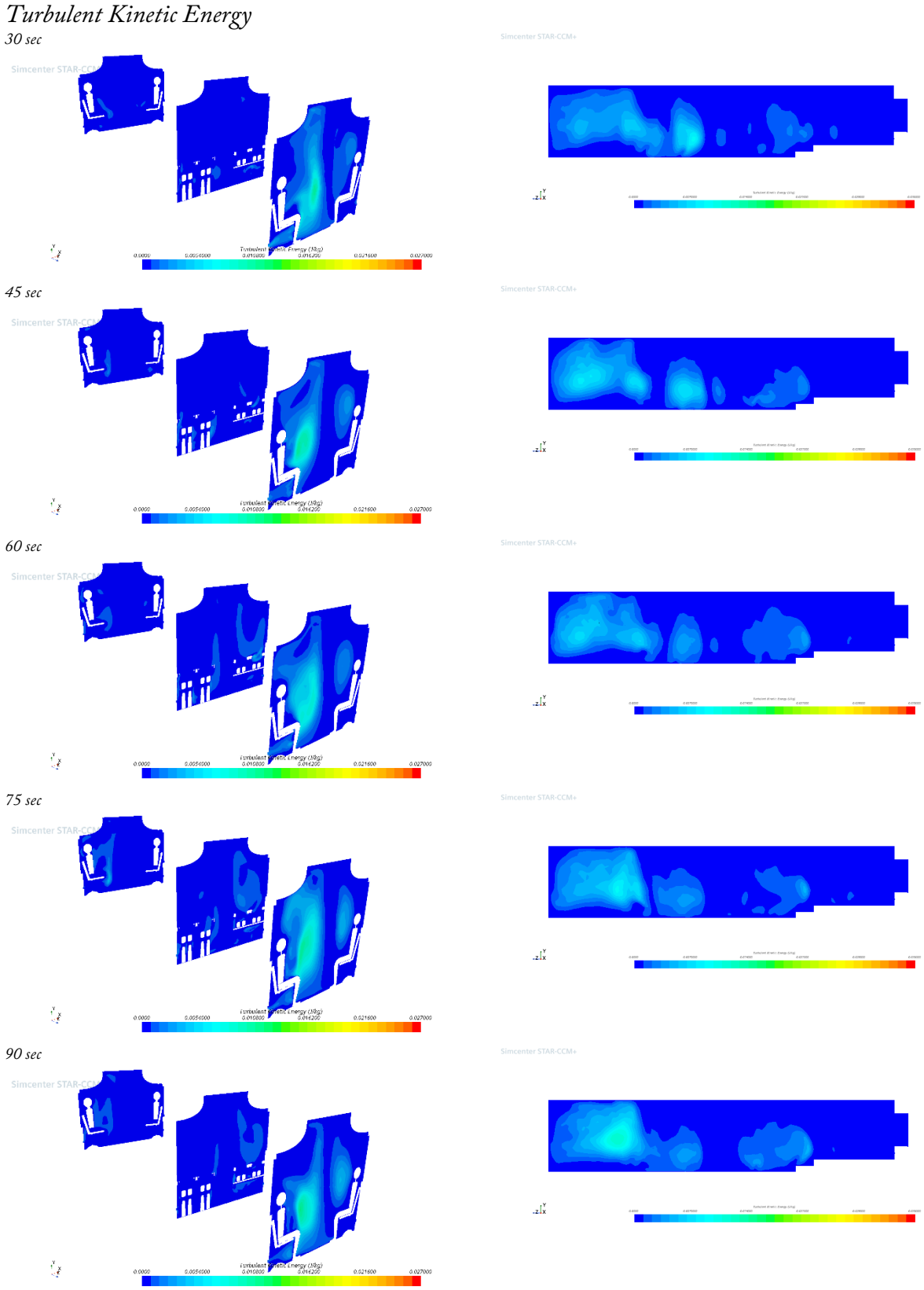

Figures 8–12 show the corresponding results when the passenger drop-off door is opened and then closed after 30 seconds. With the door opening, additional air enters the bus, and since the axial slots are at a negative pressure, there is increased air movement toward the seated passengers and the adjacent windows, especially for those sitting close to the drop-off door. When the door closes, the air movement around the passengers is gradually reduced, and at 60 seconds after the door's closure, the air movement approaches the closed-door condition identified previously.

With the opening of the door, there are sudden drops in pressure at the mid-section plane and around the passengers seated in the vicinity of the door. The pressure drops result in increased air movements at these locations and cause a non-uniformity in the air distribution further to the front of the bus. There is a gradual increase in pressure at these locations until the door is closed.

When the door is closed, there pressure increases at the mid-section plane and around the seated passengers, limiting air movements. The variation in pressure reduces significantly at 40 s after the door is closed, and at 50 s and 60 s, the pressure distribution approaches a steady state condition.

With the door open, there is an increase in the particles' dispersion toward the front of the bus, but this dispersion is limited to the side of the bus where the infectious passenger was sitting. The extent of the dispersion is beyond three rows in front of the infectious passenger. At 30 s when the door is closed, the particles have already reached the front of the bus.

When the door is closed, even though the air movement is reduced, the concentration of the particles is reduced gradually with additional dispersion toward the rows behind the infectious passenger. However, there are significant risks to the passengers sitting in the front three rows which still have a high concentration of particles.

With the opening of the door, vorticity is reduced at the mid-section plane and around the passengers due to increased mixing and reduced velocity gradients. However, after 15 seconds of the door opening, the air movement around the passengers sitting in the horizontal rows has recovered, resulting in increased vorticity at these locations. When the door is closed, there is a gradual redistribution of vorticity at the mid-section plane and around the passengers, approaching a steady state condition as in the closed-door air exchanges.

Opening the door increases TKE around passengers facing each other which extends to their feet near the floor. When the door is closed, since there is still air exchange along the axial slots, the increase in TKE is mostly around the passengers' feet. However, at 50 s, the TKE distribution is similar to the corresponding distribution before the opening of the door.

Figure 8. Contours of Mean Velocity in Open-Closed Door Conditions

Door open Velocity

5 sec before

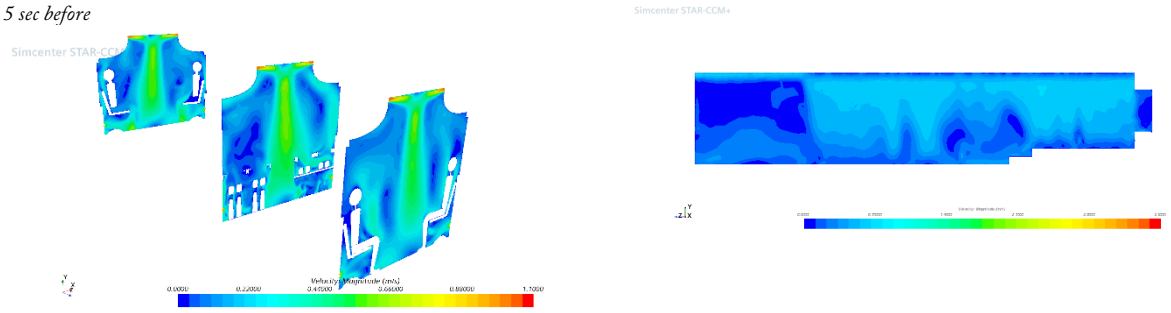

Door Open

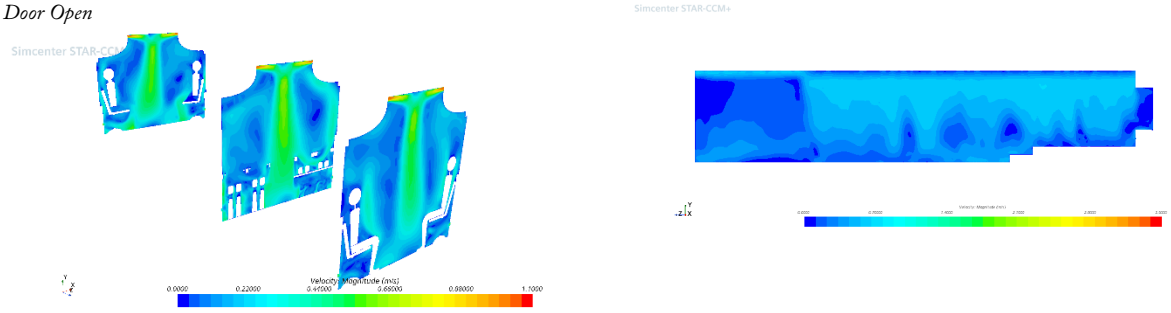

5 sec after Door Open

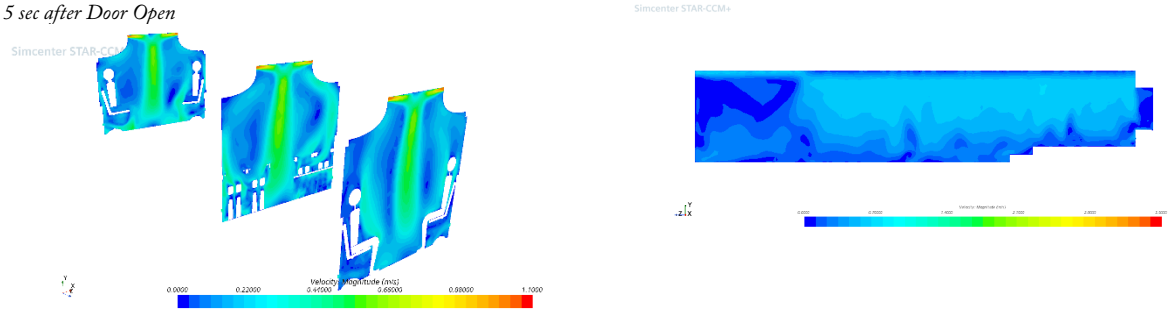

15 sec

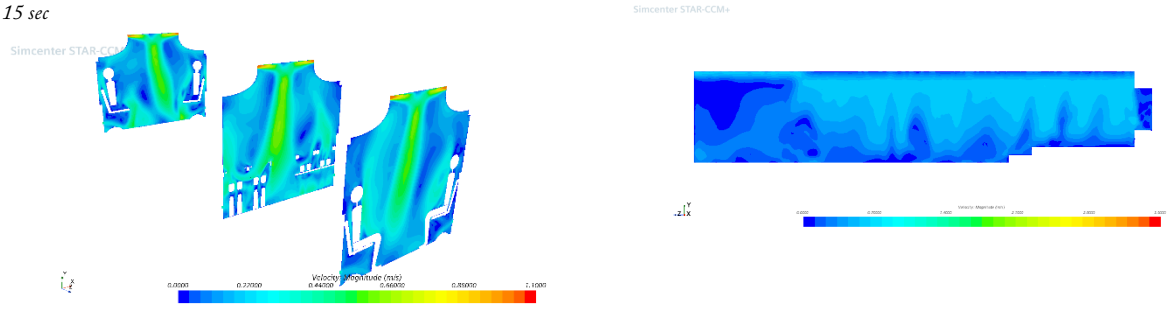

25 sec

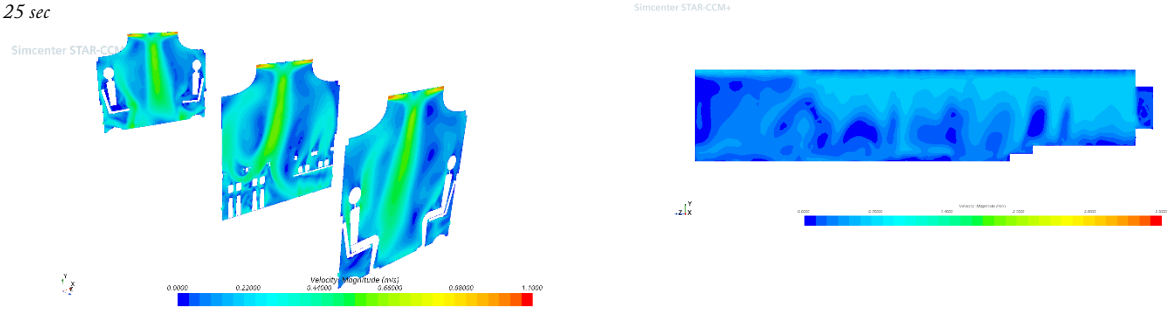

30 sec (Door Closed)

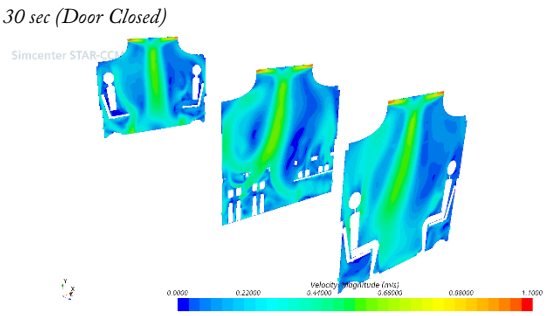

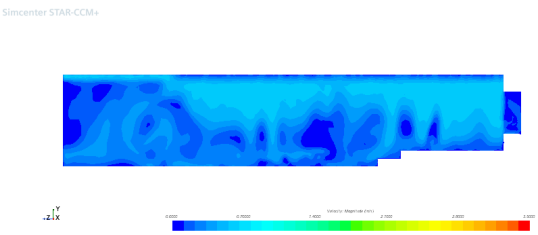

35 sec

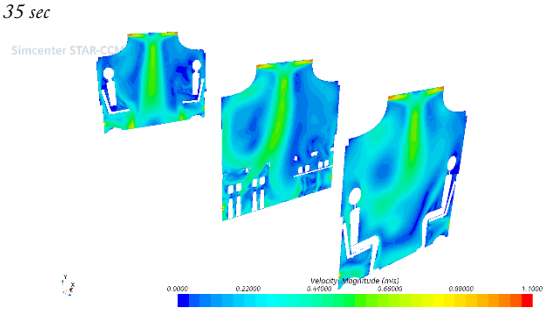

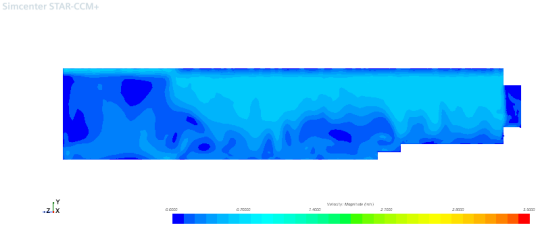

40 sec

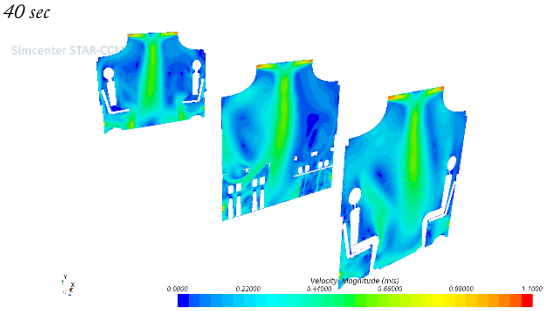

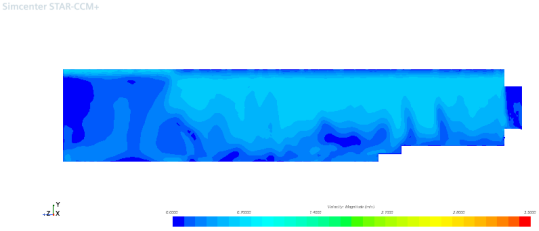

50 sec

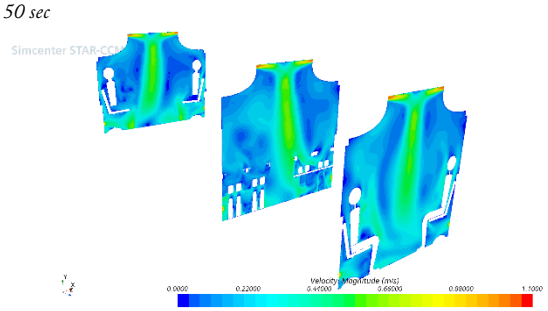

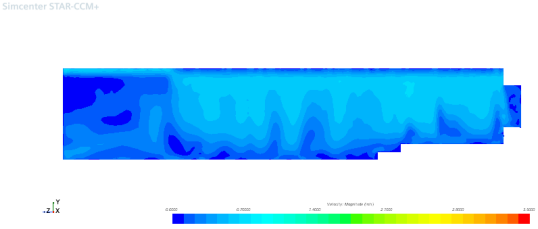

60 sec

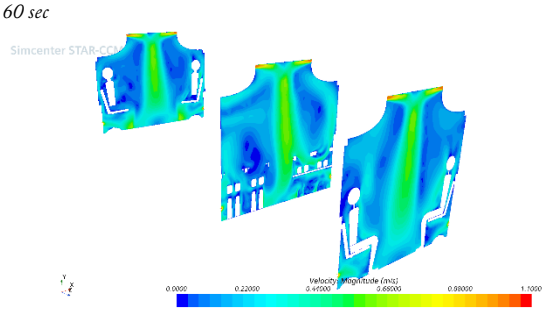

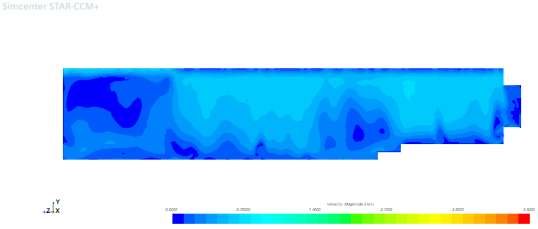

Figure 9. Contours of Mean Pressure in Open-Closed Door Conditions

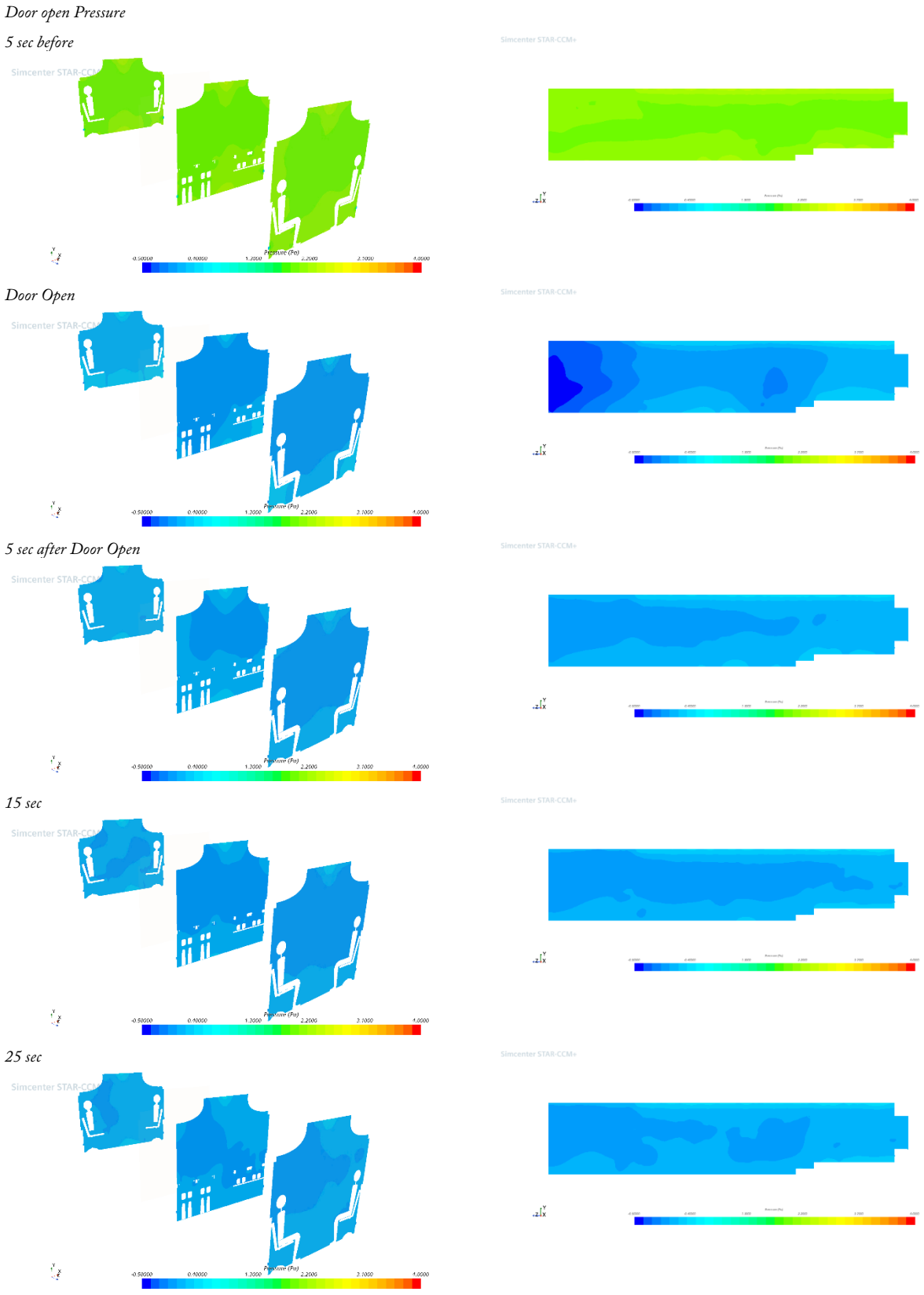

30 sec (Door Closed)

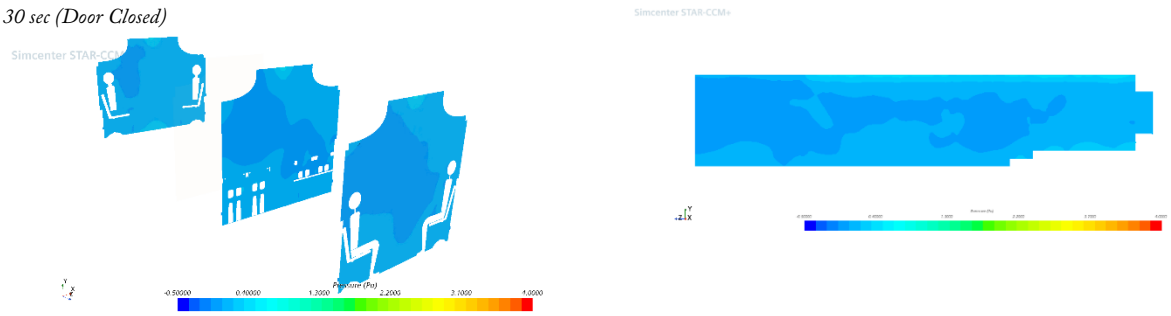

35 sec

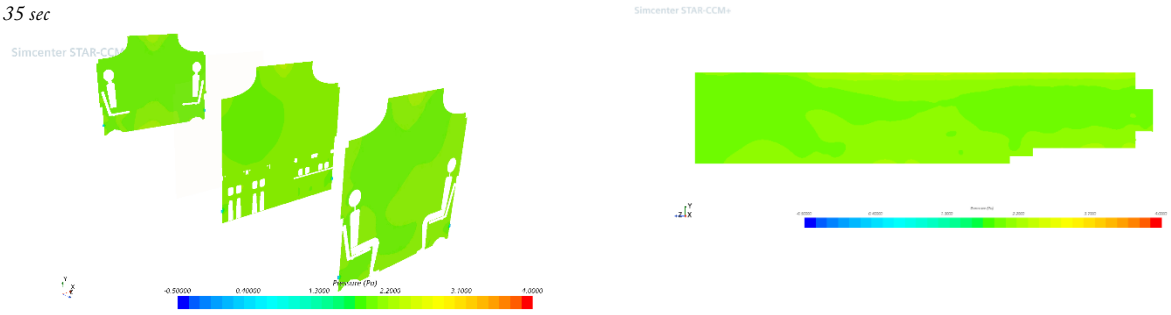

40 sec

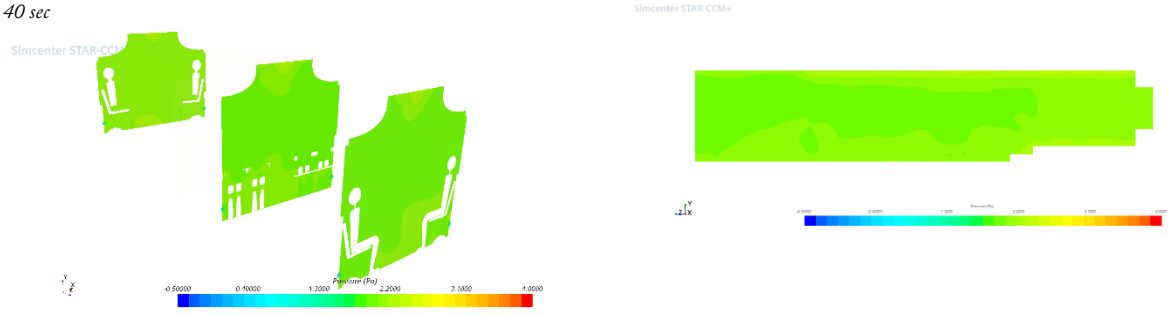

50 sec

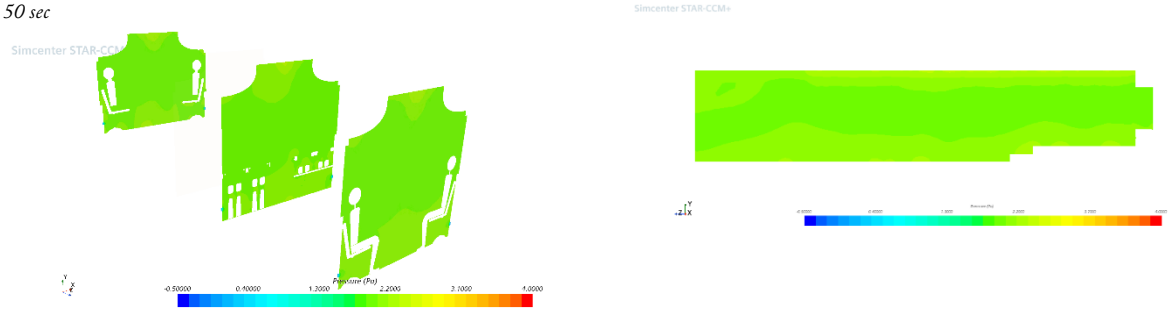

60 sec

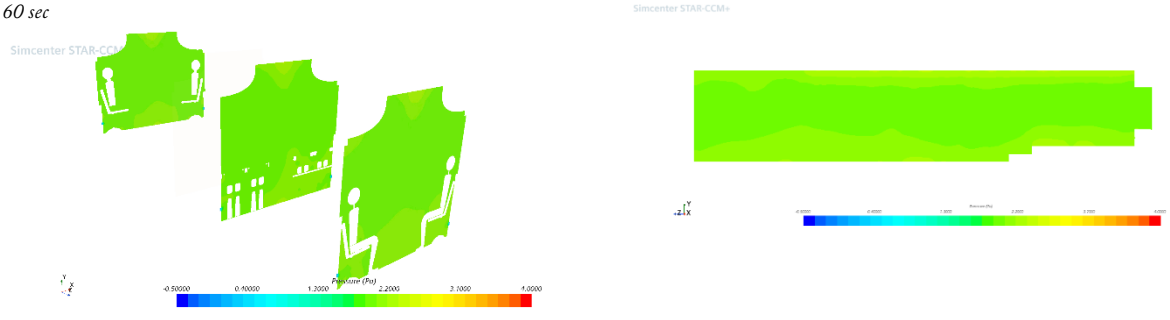

Figure 10. Particles' Dispersion in Open-Closed Door Conditions

Door open Particles

5 sec before

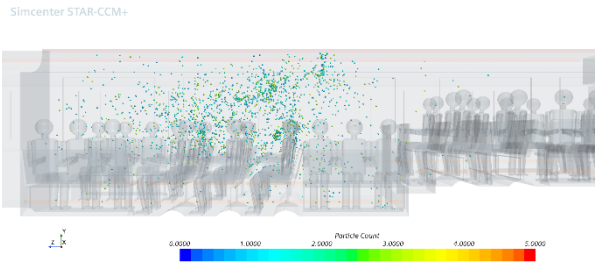

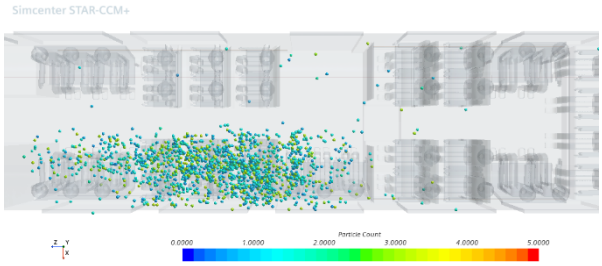

Door Open

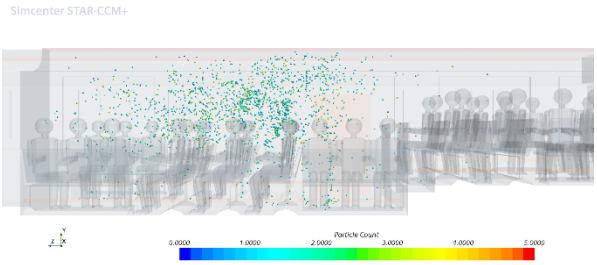

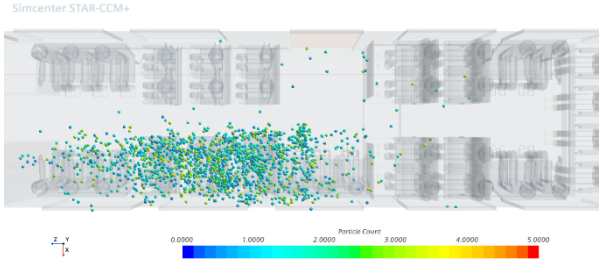

5 sec after Door Open

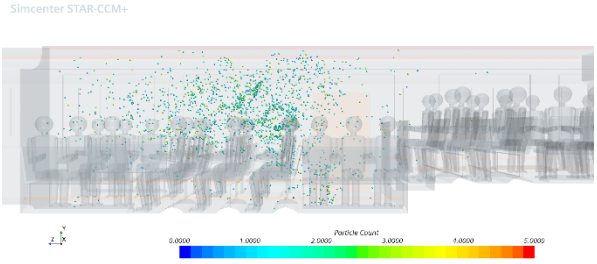

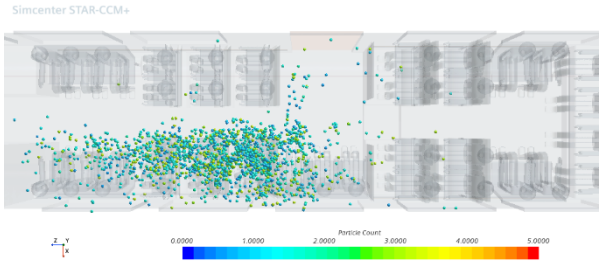

15 sec

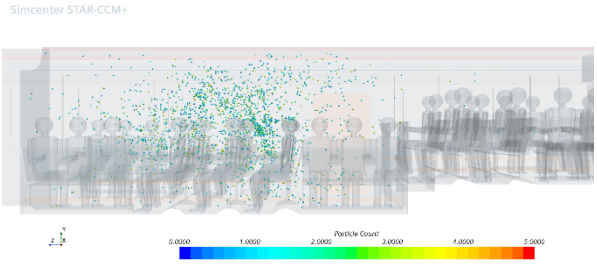

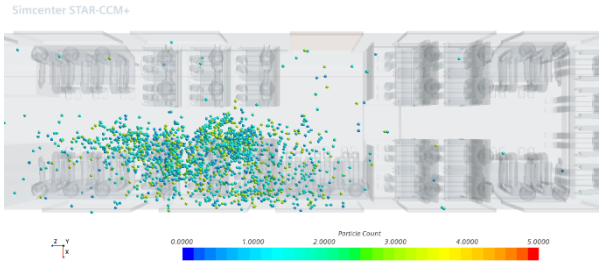

25 sec

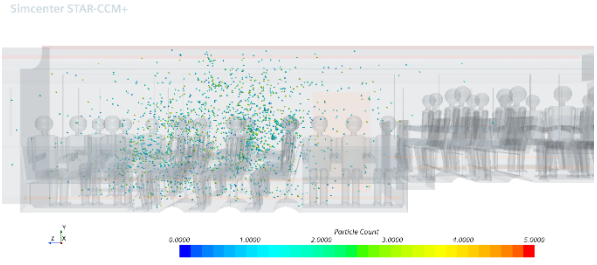

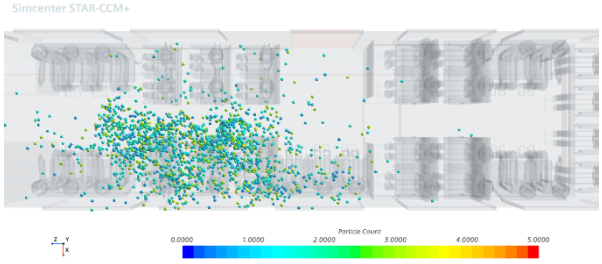

30 sec (Door Closed)

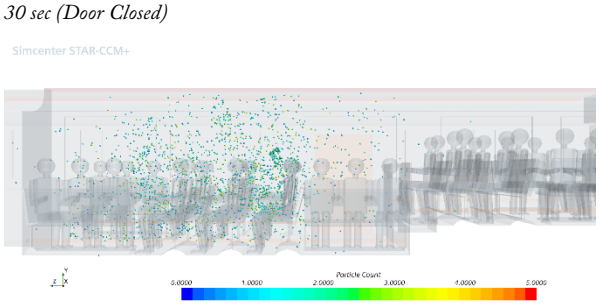

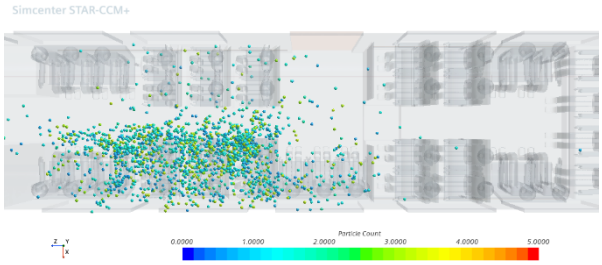

35 sec

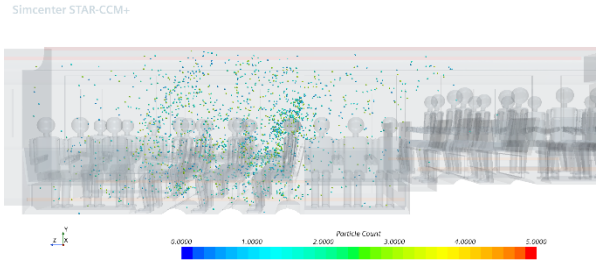

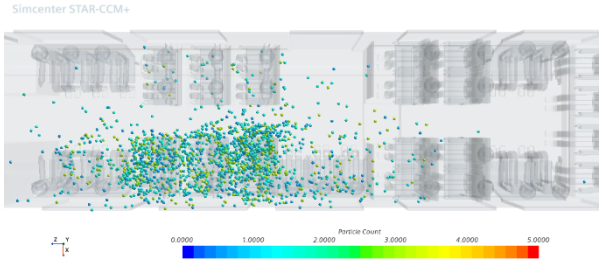

40 sec

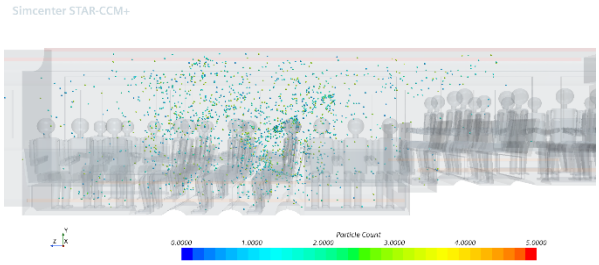

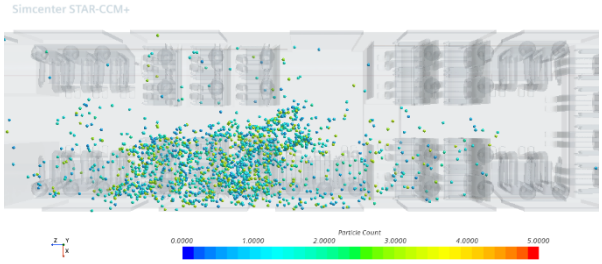

50 sec

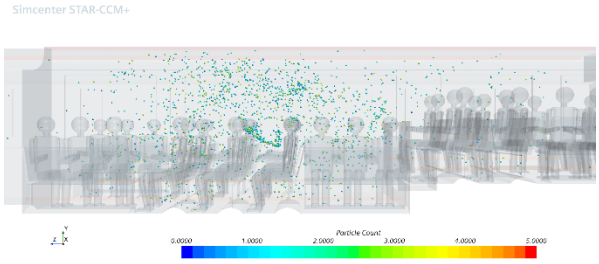

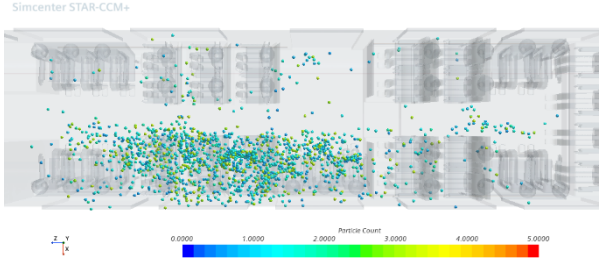

60 sec

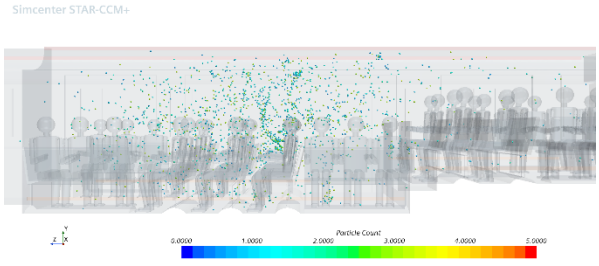

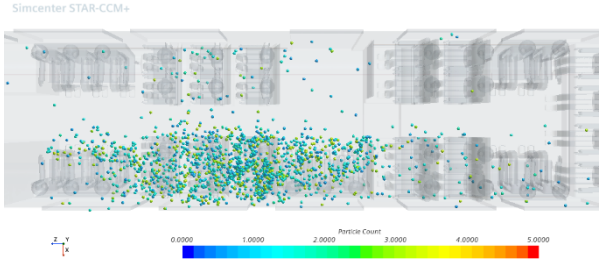

Figure 11. Contours of Axial Vorticity in Open-Closed Door Conditions

Door open Vorticity

5 sec before

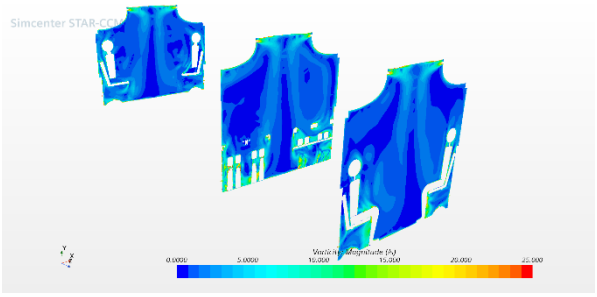

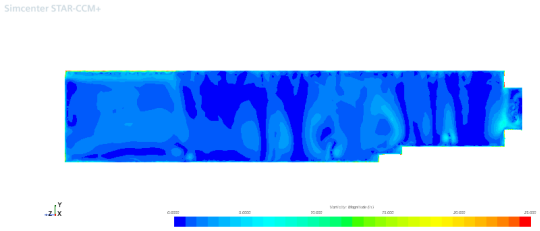

Door Open

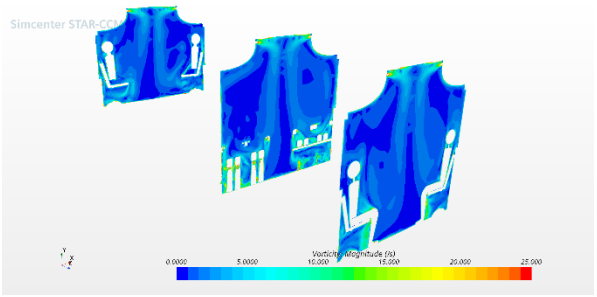

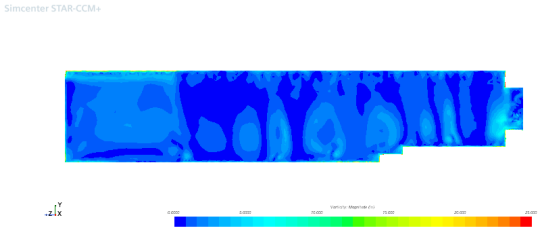

5 sec after Door Open

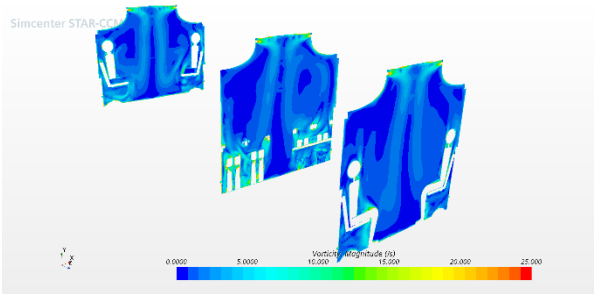

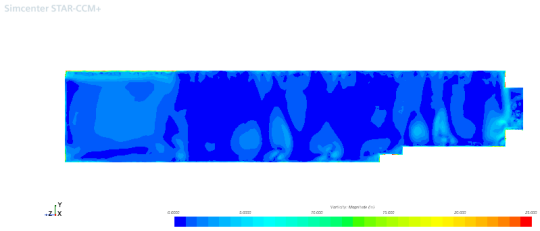

15 sec

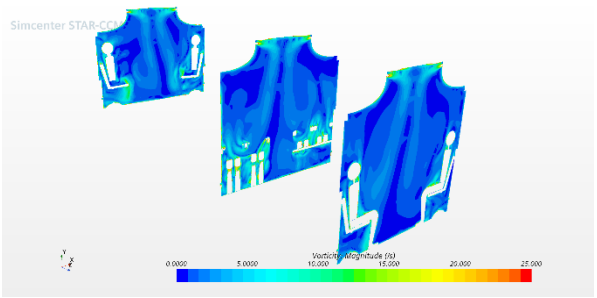

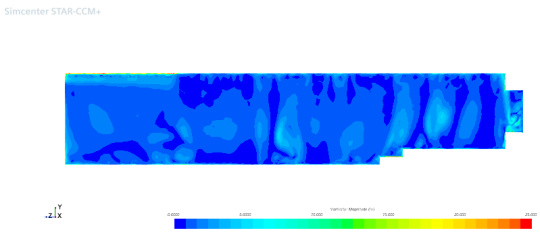

25 sec

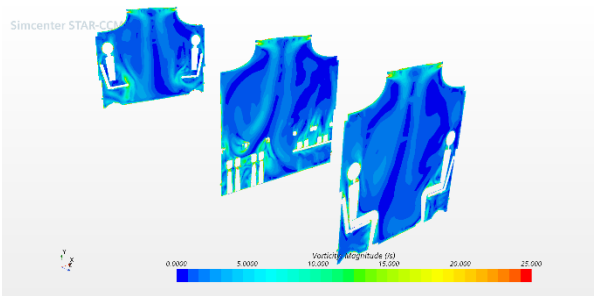

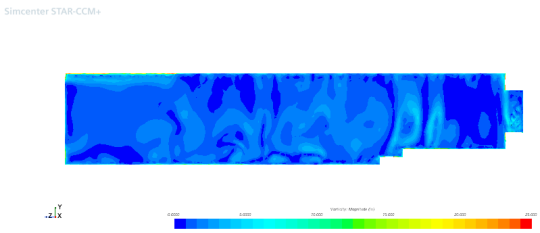

30 sec (Door Closed)

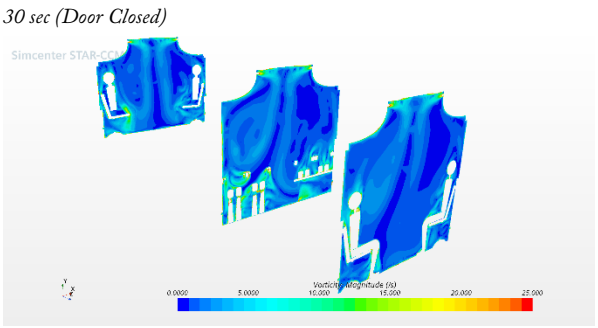

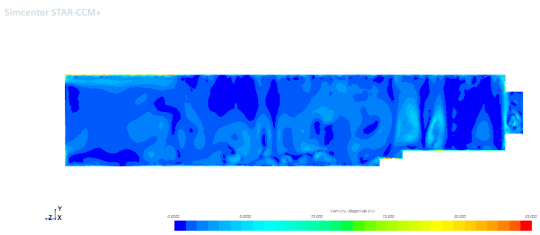

35 sec

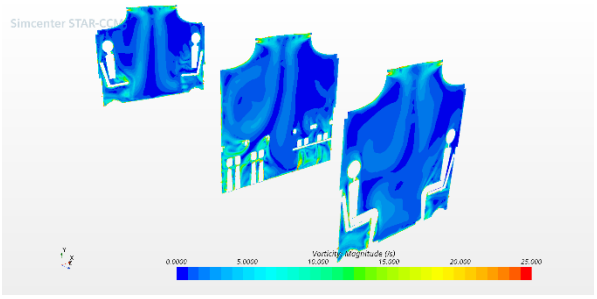

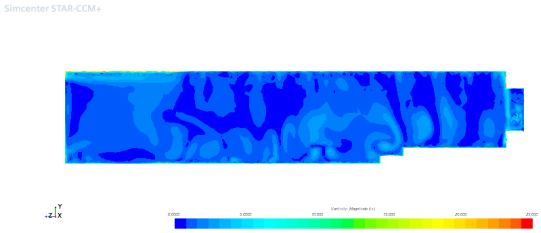

40 sec

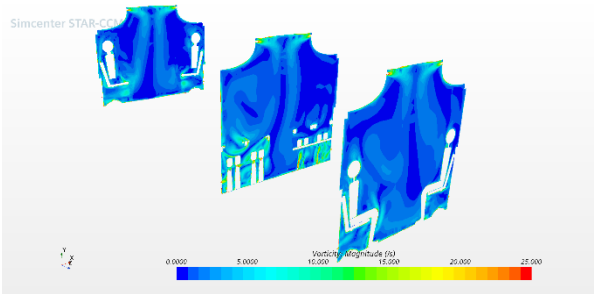

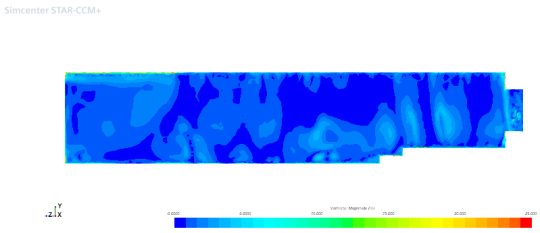

50 sec

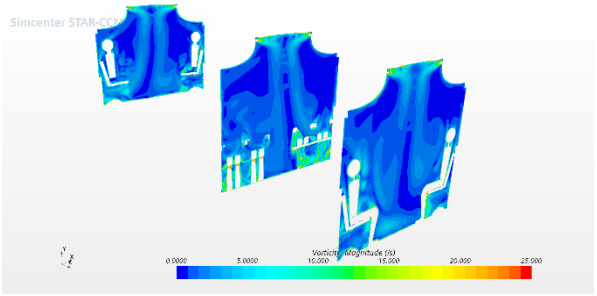

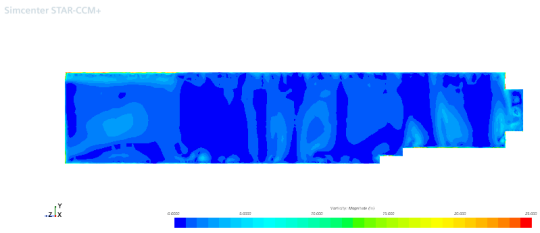

60 sec

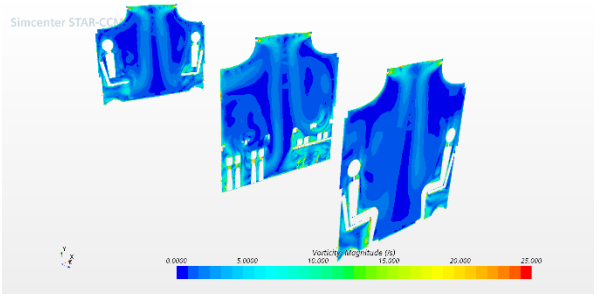

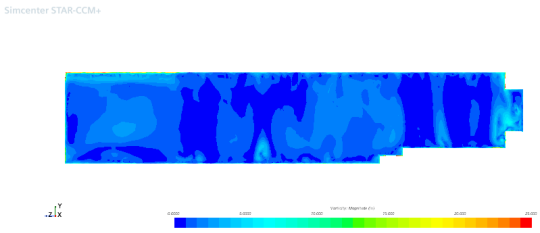

Figure 12. Contours of TKE in Open-Closed Door Conditions

Door open Turbulent Kinetic Energy

5 sec before

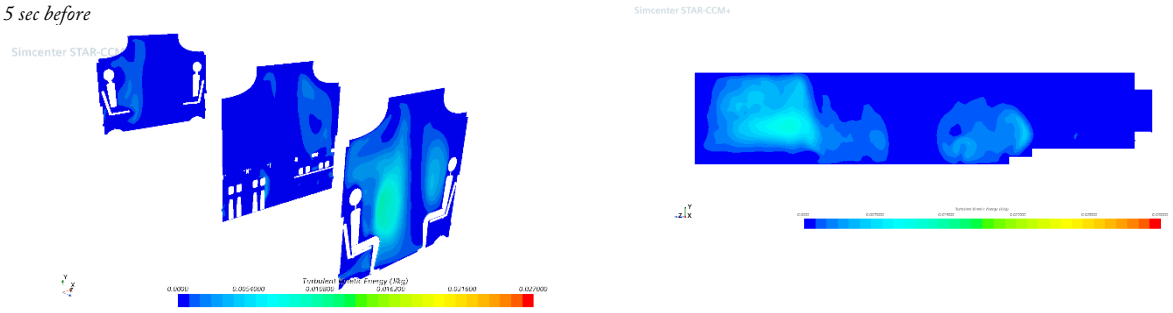

Door Open

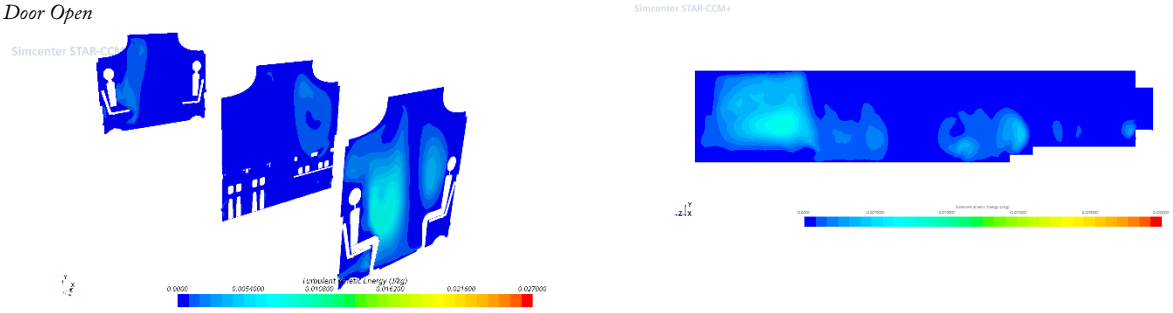

5 sec after Door Open

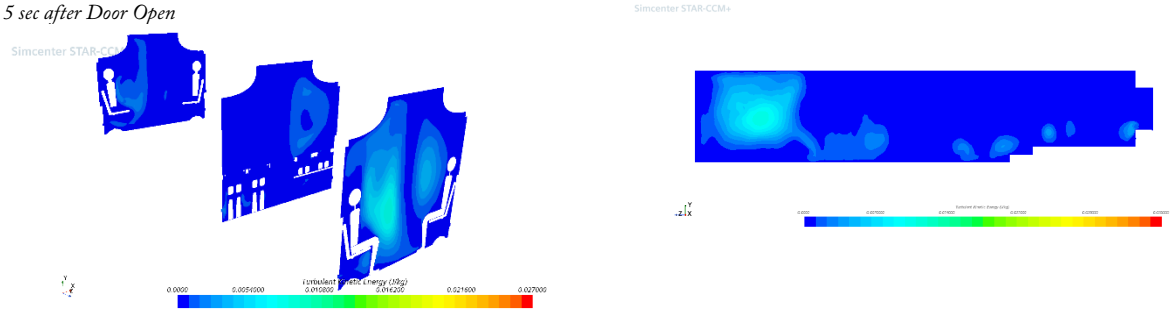

15 sec

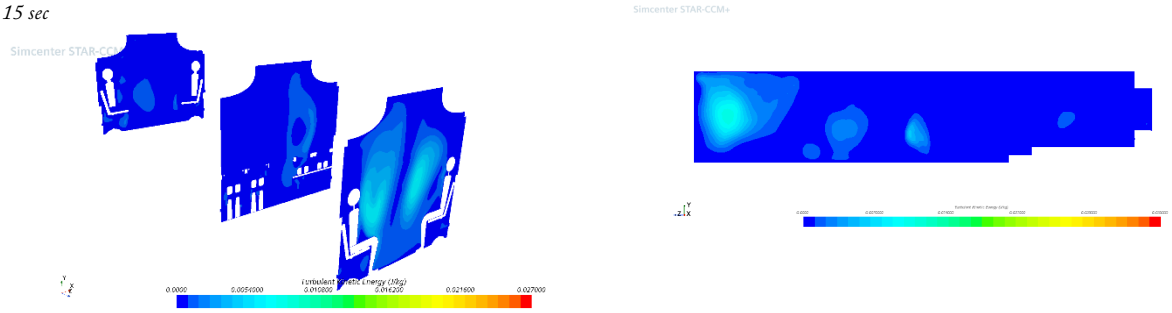

25 sec

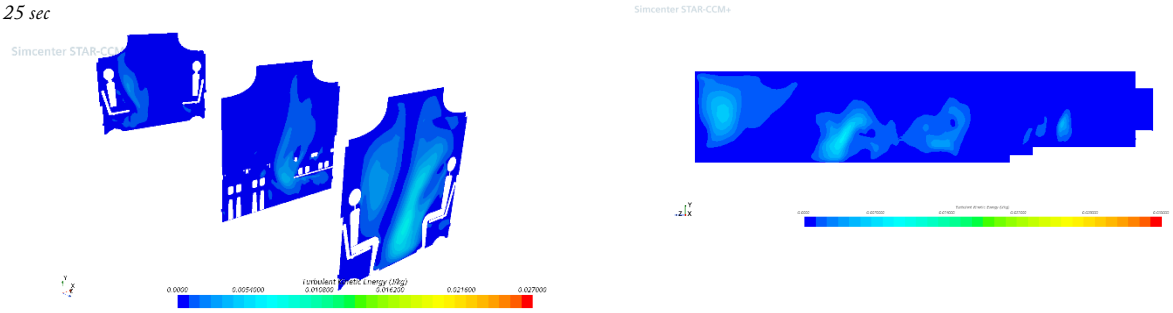

30 sec (Door Closed)

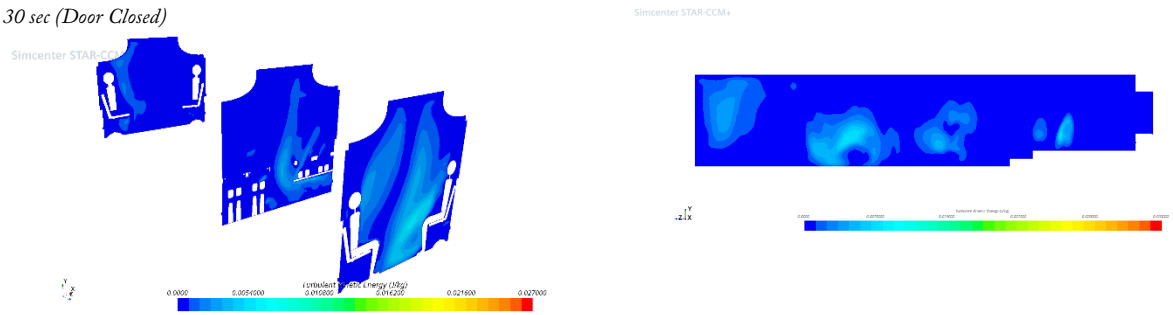

35 sec

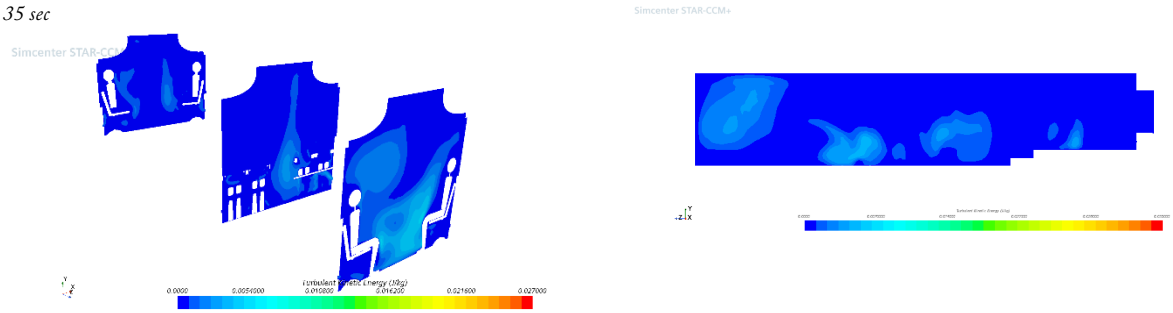

40 sec

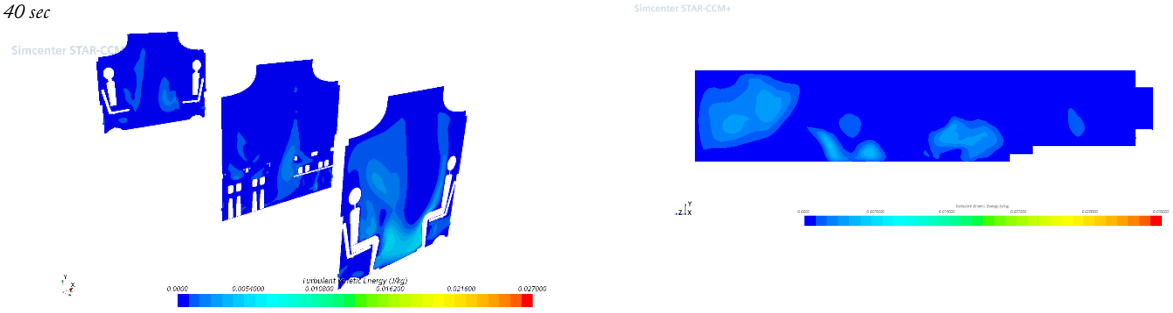

50 sec

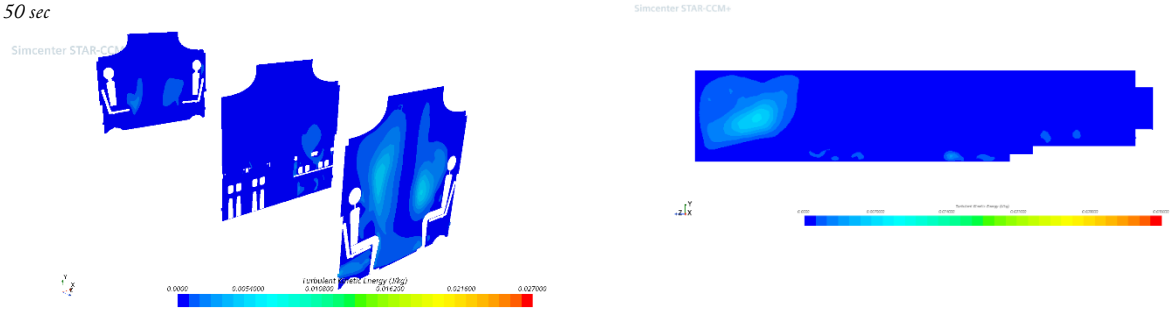

60 sec

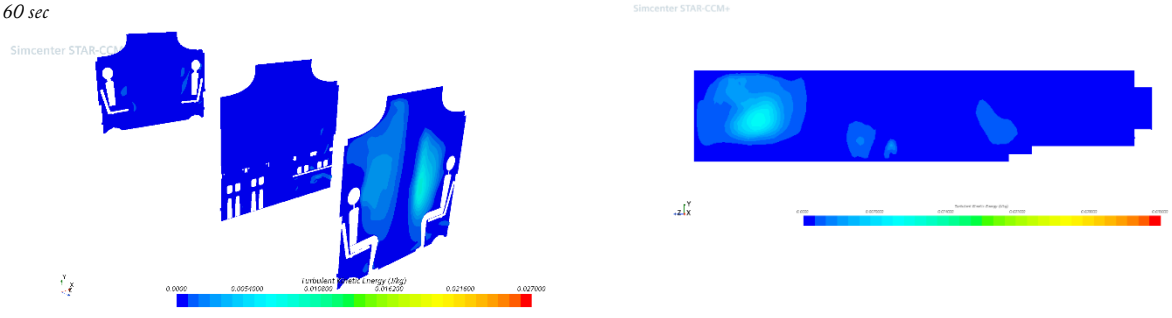

3.2 The Vertical Exhausting Slots

Figures 13–17 show the contours of the mean velocity and pressure, the particles' dispersion, the contours of the vorticity, and the TKE at the mid-section plane and monitoring areas for vertical slots air exchange with the closed drop-off door. The vertical slots have reduced air exchange at the foot of the passengers near the floor with more air movements toward the passengers' faces and the adjacent windows. There are more air movements at the mid-section plane, and at these locations, pressure is low. There is a slight increase in pressure near the passengers' feet which corresponds to the low air exchanges at these locations.

Particle dispersion is reduced significantly with the vertical exhausting slots. The front rows of the infectious passengers are not impacted, and the dispersion is toward the passengers sitting in the rear seats with some particles crossing the aisle toward the other side of the bus. This is in line with increased air movement around the passengers' faces and at the mid-section plane. Moreover, having more slots increases air exchange on this side of the bus.

The vertical slots and increased air movements toward the sides of the windows result in increased vorticity at these locations. For the face-to-face passengers, the increase in vorticity is seen between the passengers from the floor up. With increased vorticity, TKE is increased, and the increase is more pronounced when there are obstruction and velocity gradients.

Figure 13. Contours of Mean Velocity with a Closed Door

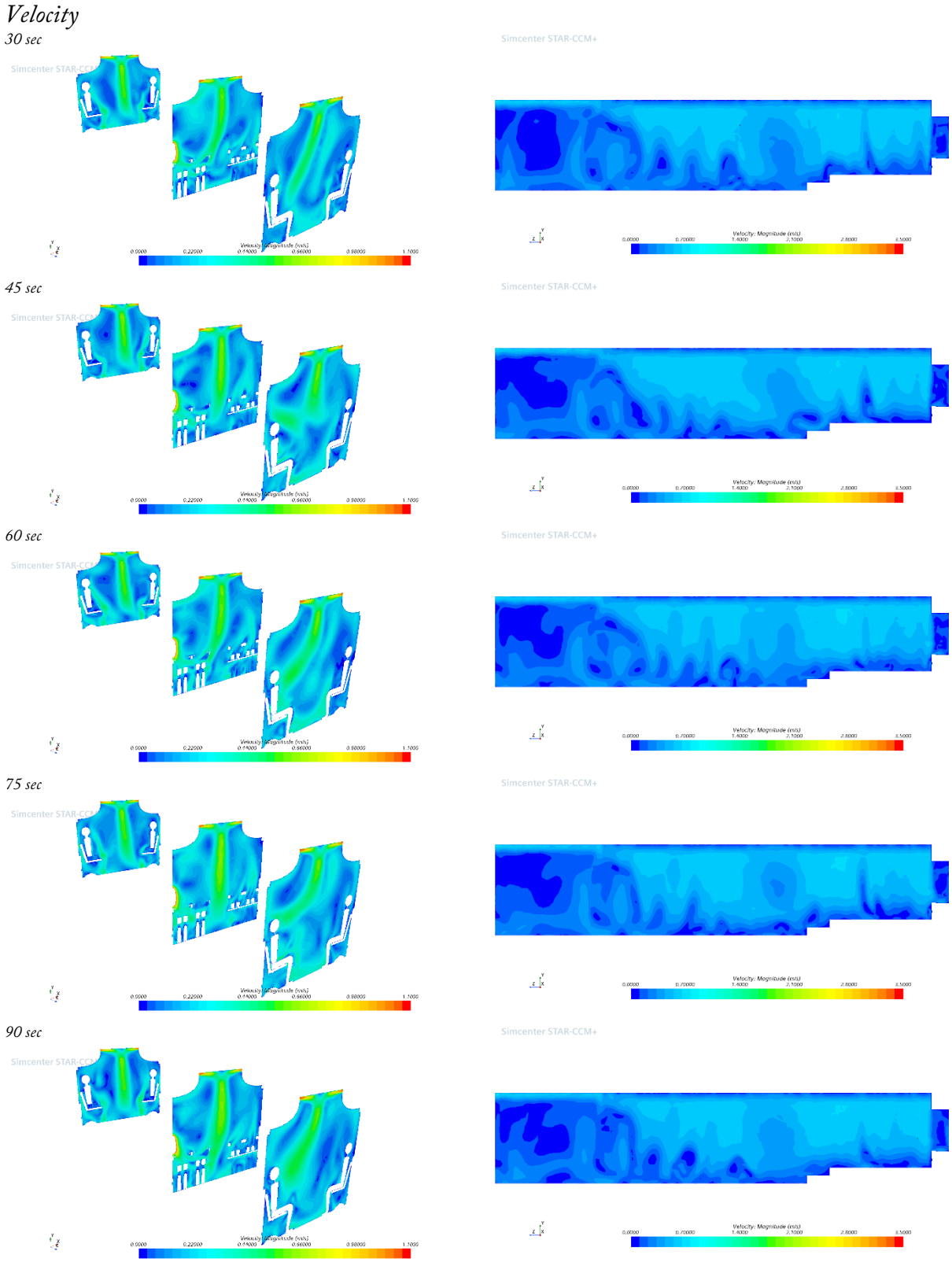

Figure 14. Contours of Mean Pressure with a Closed Door

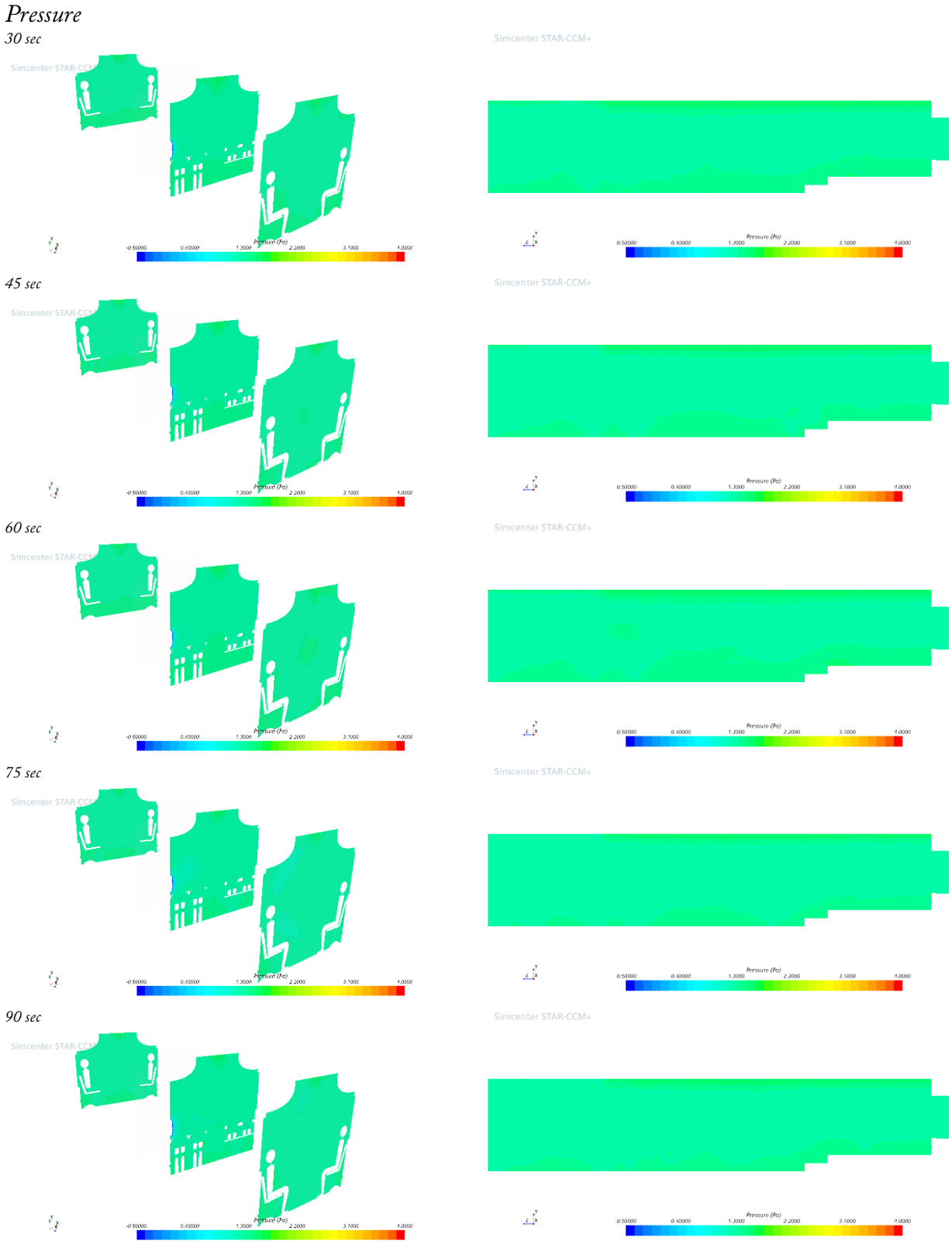

Figure 15. Particles' Dispersion with a Closed Door

Particles

30 sec

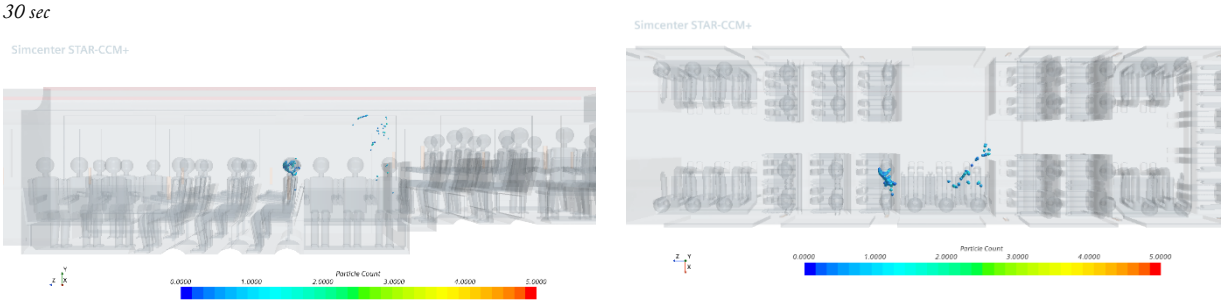

45 sec

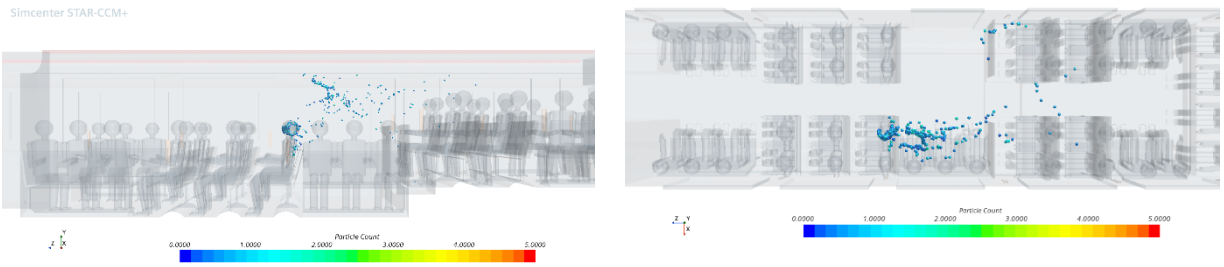

60 sec

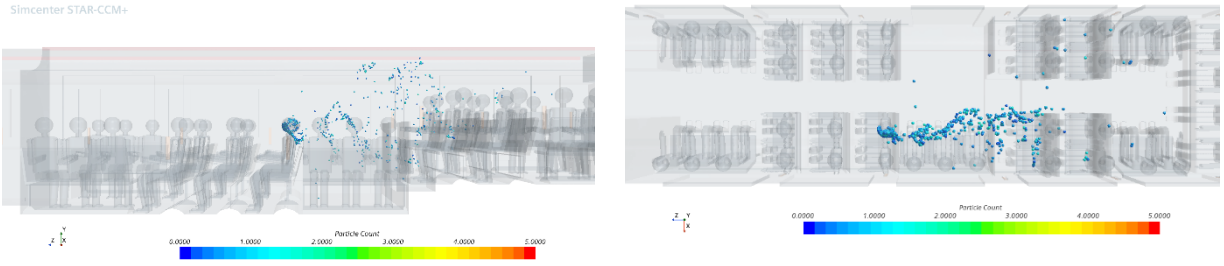

75 sec

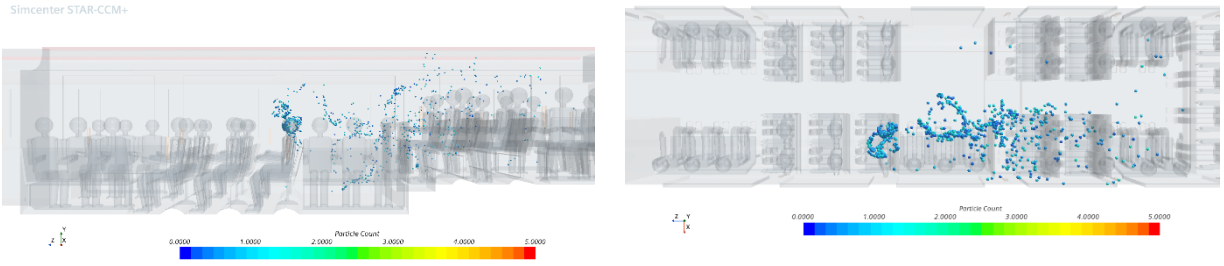

90 sec

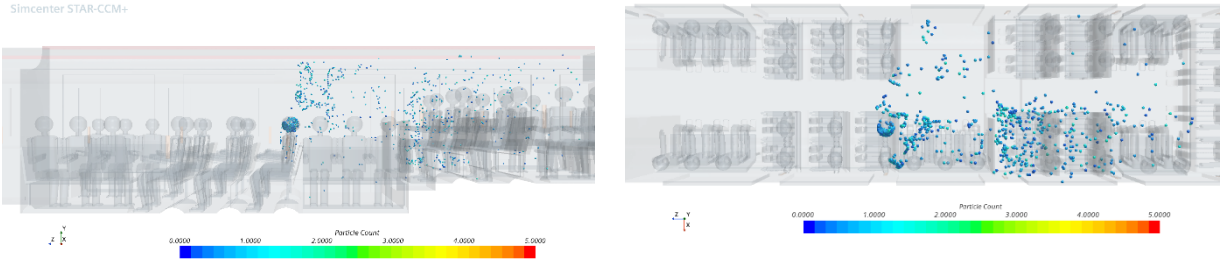

Figure 16. Contours of Axial Vorticity with a Closed Door

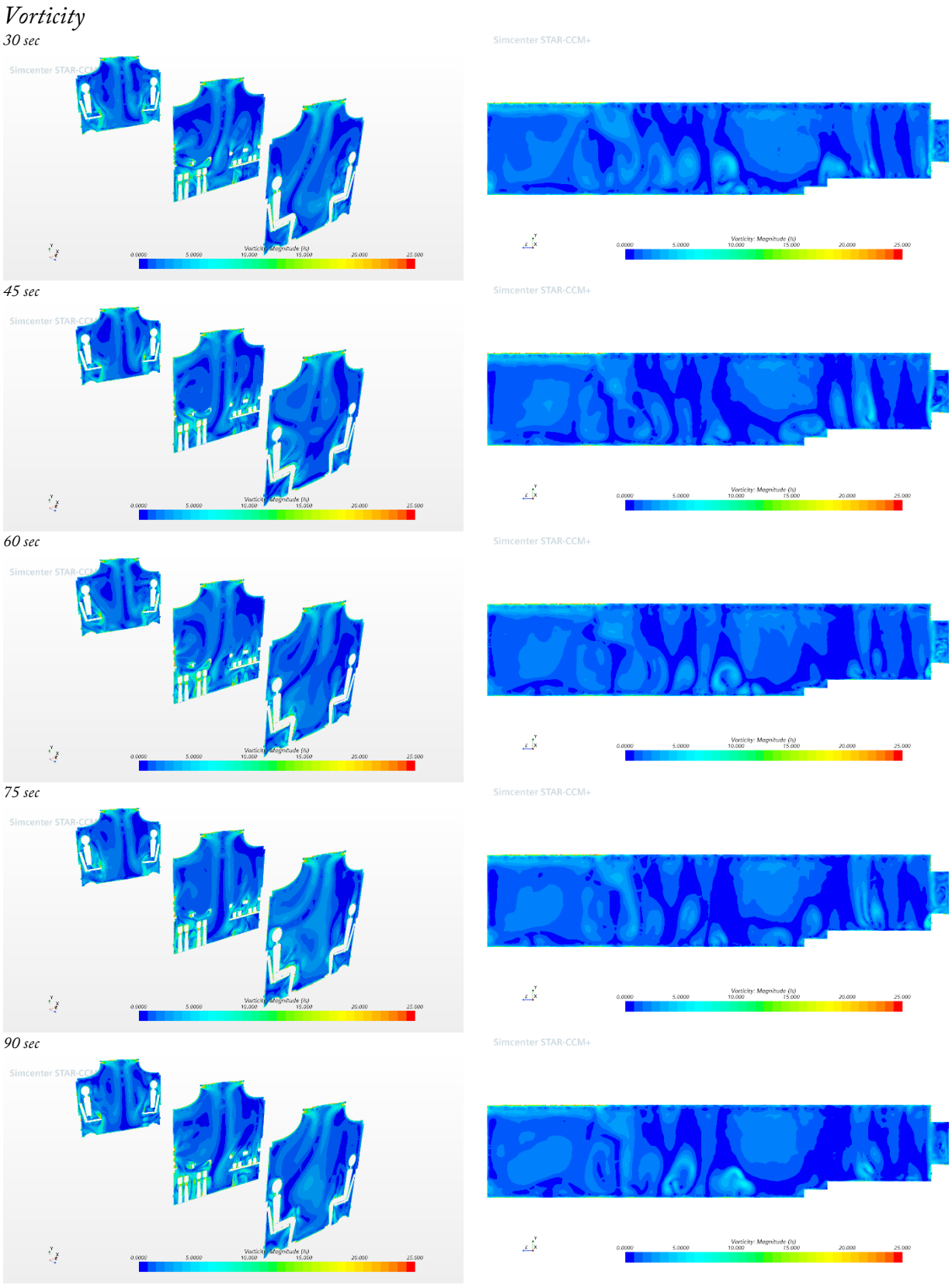

Figure 17. Contours of TKE with a Closed Door

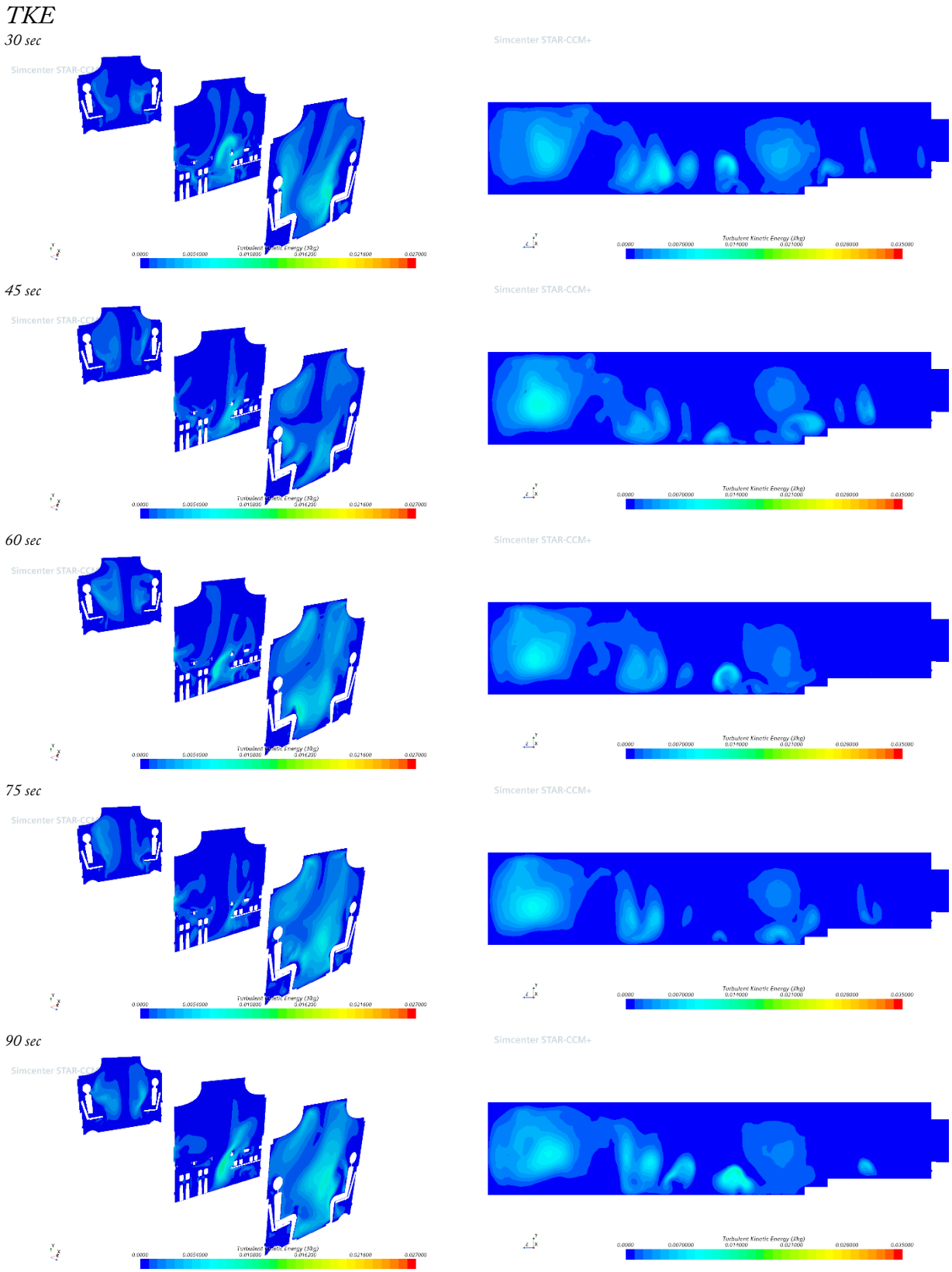

Figures 18–22 show the corresponding results with the door opened for 30 seconds and then closing. As before, the opening of the door results in increased air intake into the bus and high air movement toward the vertical slots. Since the vertical slots are significantly above the floor, the increased air movement is mostly toward the upper half of the passengers' bodies. This effect is mostly seen for the passengers sitting close to the door and the back. Toward the front of the bus, the air movement is still similar to before the drop-off door opened with downward flow from the ceiling slots, tilting toward the vertical slots at specific locations, and impacting air movement at the faces of the passengers sitting at these locations. When the door is closed, the air movement gradually approaches the steady state solution, as seen before the opening of the drop-off door, but the process is slow, and by 60 seconds after door closure, the changes are still in a transient state.

The pressure drops with the opening of the door at the mid-section plane show areas of very low pressure. With the additional air movement toward the vertical slots, especially for those passengers sitting close to the door, a further reduction in the mean pressure is observed. With the closing of the door, pressure recovers and approaches the steady-state condition.

The impact of the open door is seen as increasing particle dispersion toward the back of the bus with some crossing over to the other side toward the door and the back. These solid particles behave as small solid spheres, and their drags are impacted by the local pressure distribution and air movement. The non-uniformity in air movement and the distribution of pressure results in further dispersion in the back area. After the door is closed, the particle concentration is reduced with an increased dispersion and air exchange, except there is still a higher concentration around the seats behind the infectious passenger. At 30 seconds after the door's closure, passengers sitting in the last half of the bus are all exposed to the virus, although the concentration and the number of particles that each passenger is exposed to is significantly decreased.

Increased vorticity is seen toward the passengers sitting across the door when the door is opened. The variation of vorticity is related to the level of obstruction and the corresponding velocity gradients at each location. With the door open, for passengers facing each other, there are increases in vorticity around the passengers' lower half of the body which expands into the mid-section plane. For the horizontal sitting passengers, the increase in air exchange due to the door opening results in increased vorticity around the upper passengers' bodies toward the vertical slots.

With the door opened, increased TKE is seen toward the front of the bus, but with the closing of the door, TKE increases become localized and are related to the local obstructions and velocity fluctuations. Both vorticity and TKE play a role in the level of concentration and exhaust rate of the particles.

Figure 18. Contours of Mean Velocity in Open-Closed Door Conditions

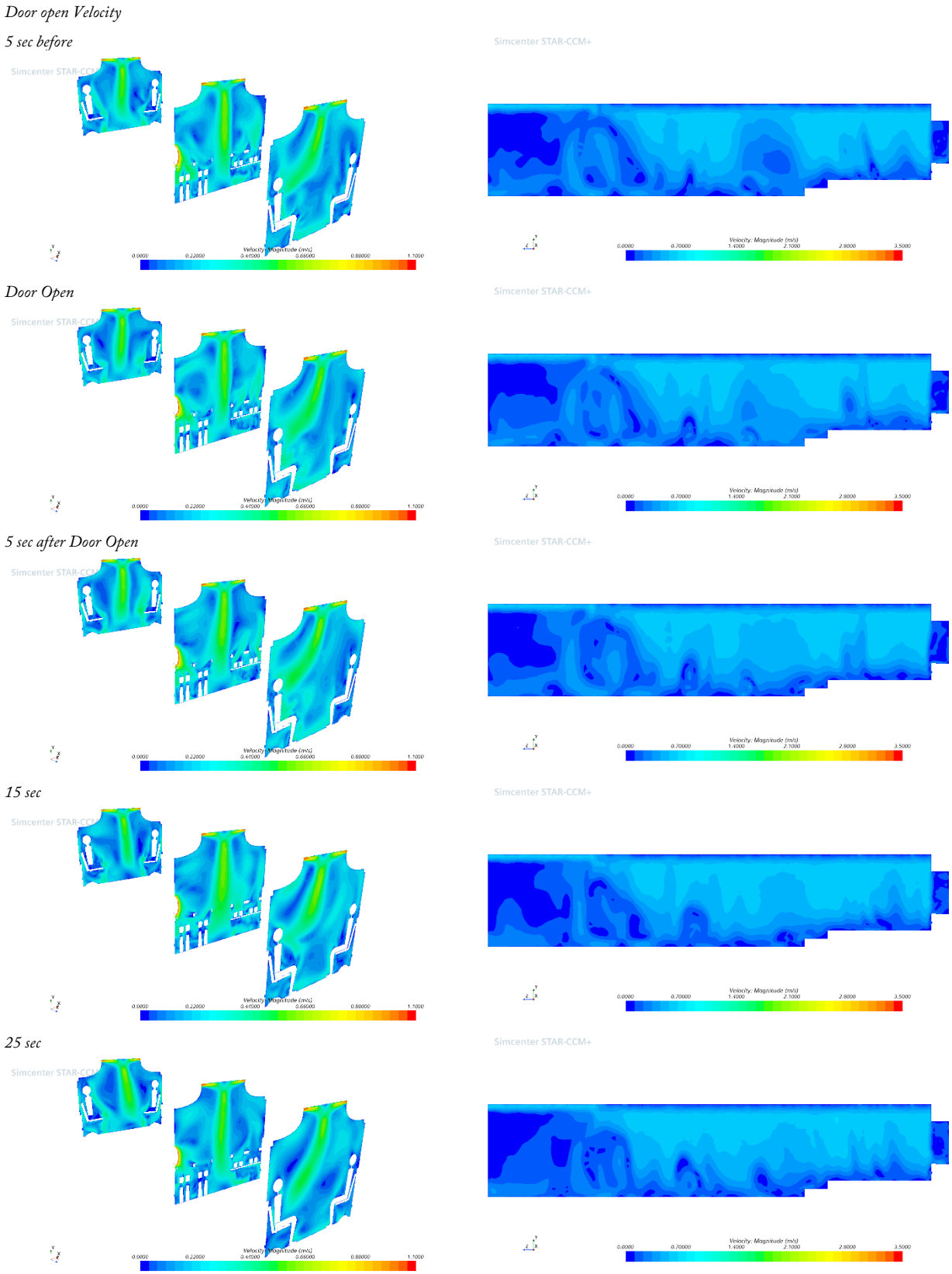

30 sec (Door Closed)

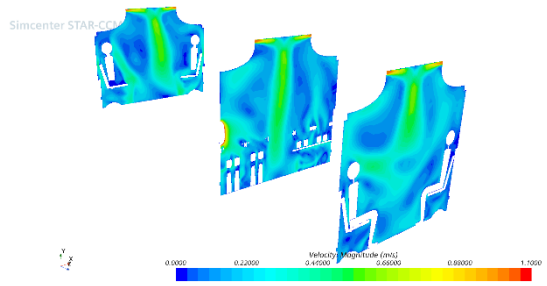

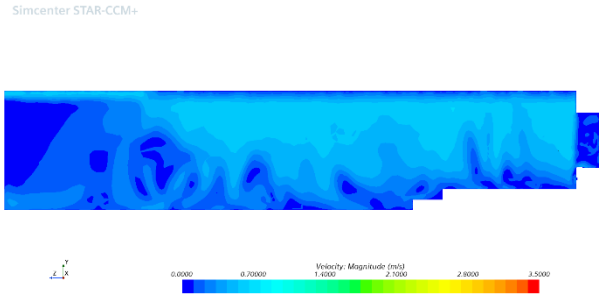

35 sec

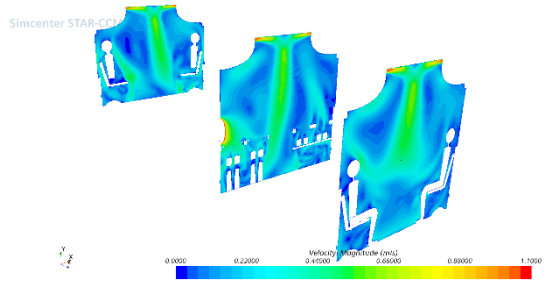

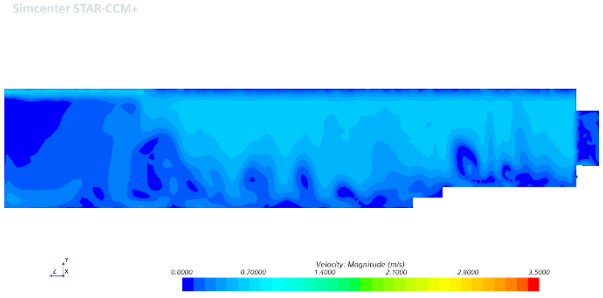

40 sec

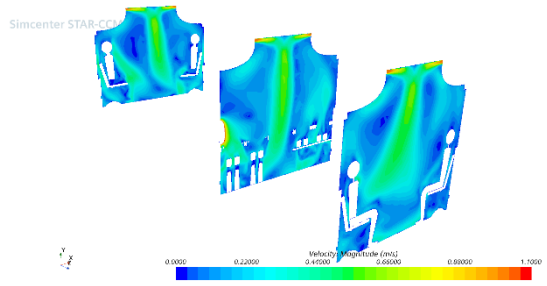

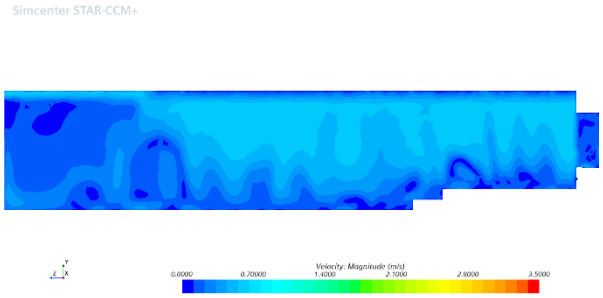

50 sec

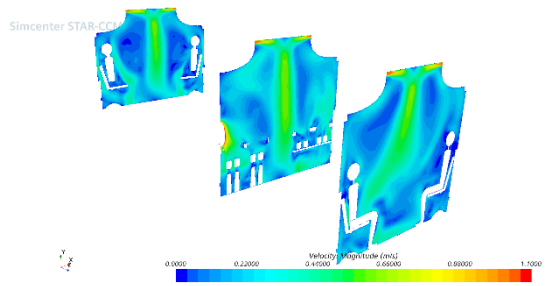

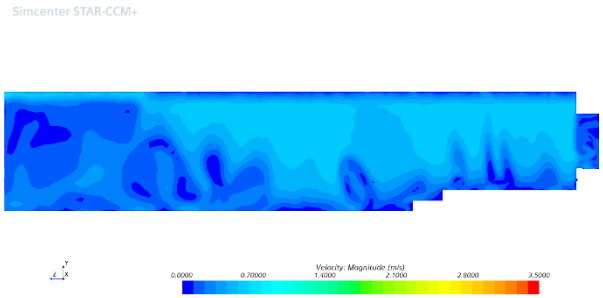

60 sec

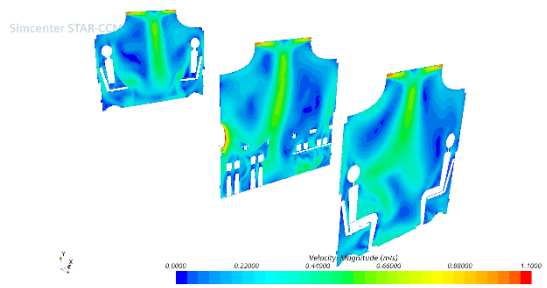

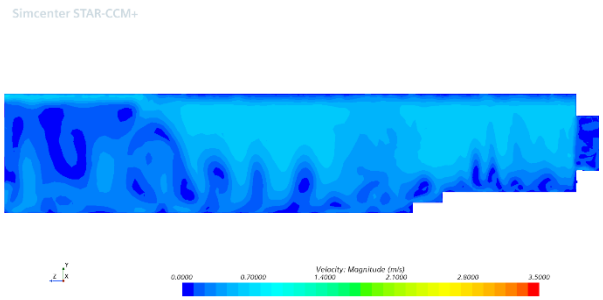

Figure 19. Contours of Mean Pressure in Open-Closed Door Conditions

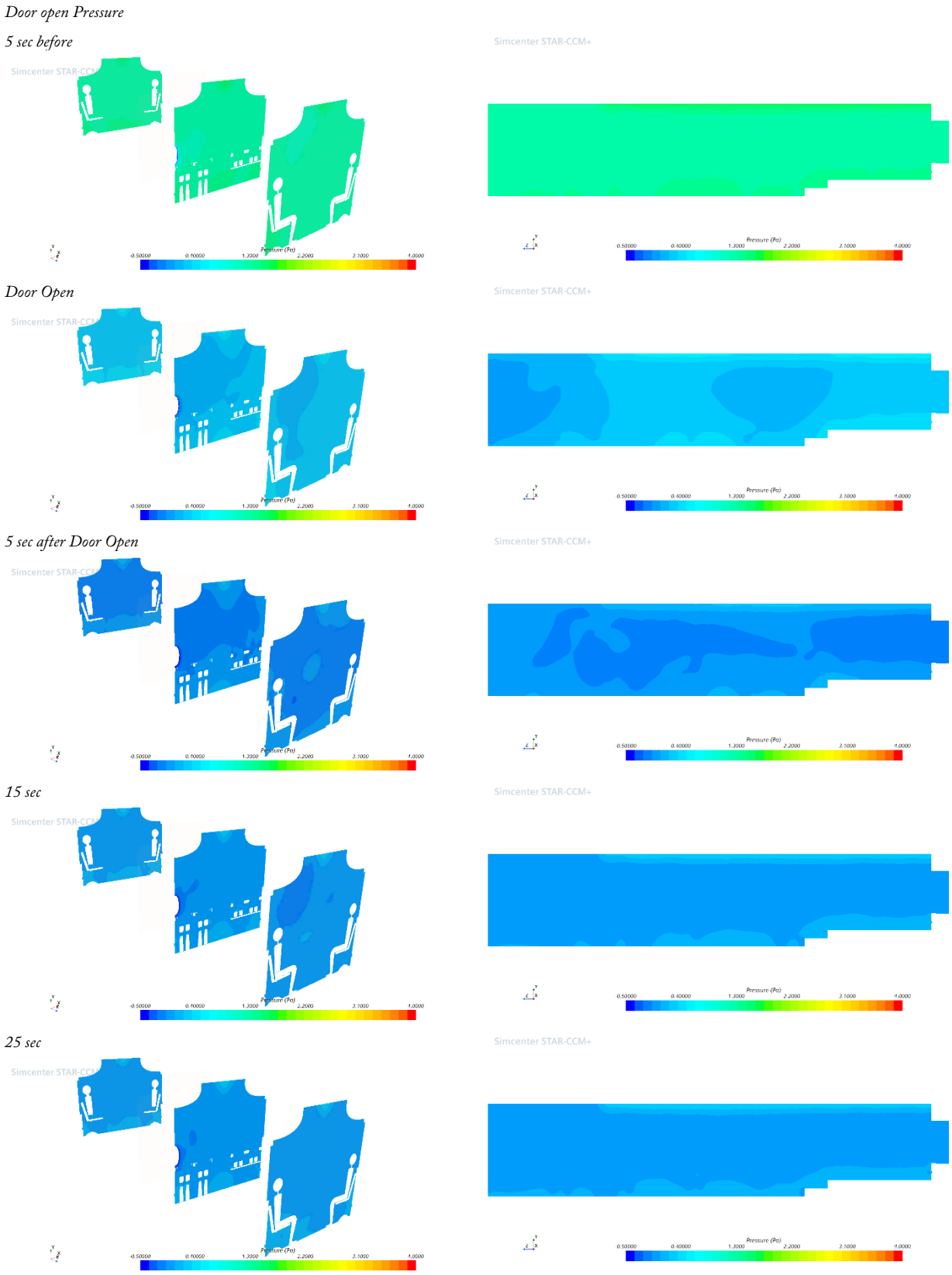

30 sec (Door Closed)

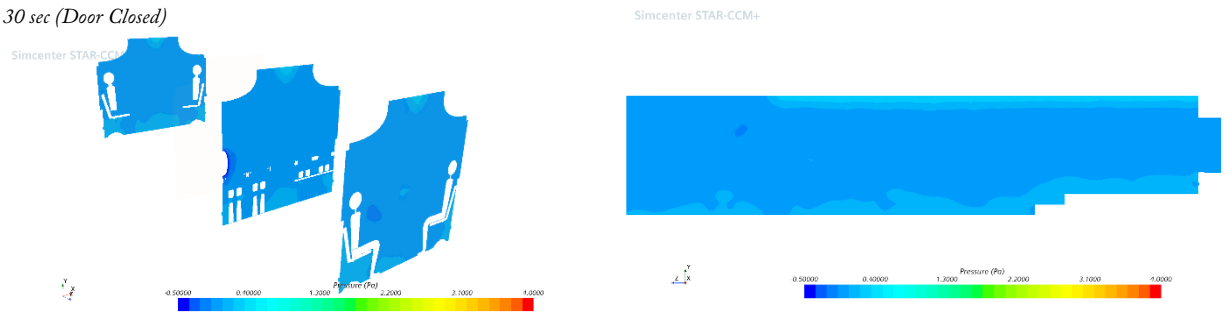

35 sec

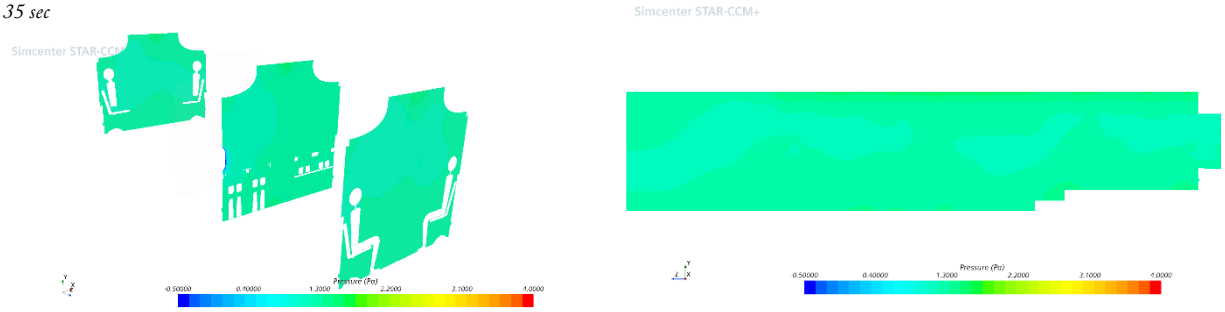

40 sec

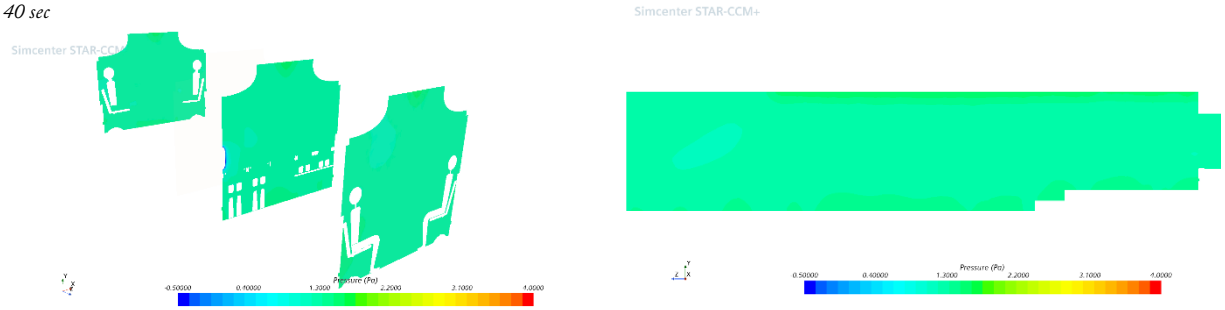

50 sec

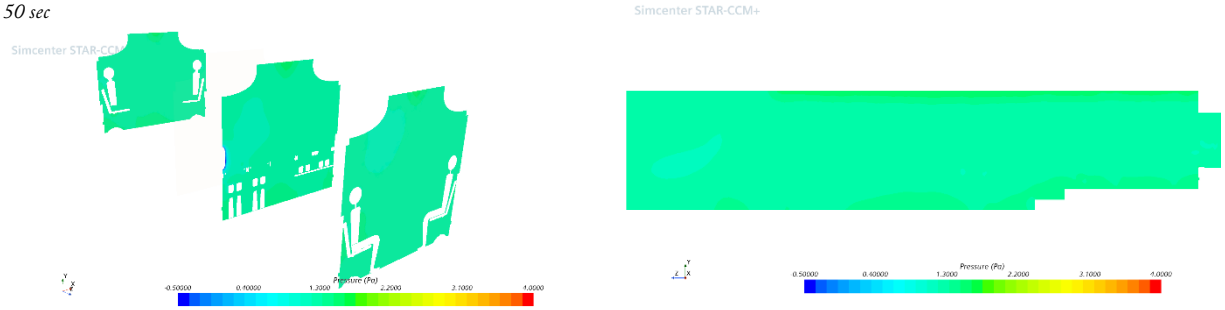

60 sec

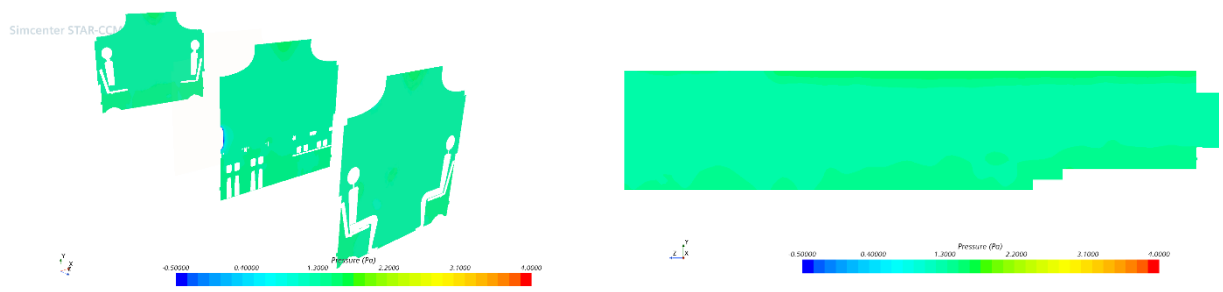

Figure 20. Particles' Dispersion in Open-Closed Door Conditions

Door open Particles

5 sec before

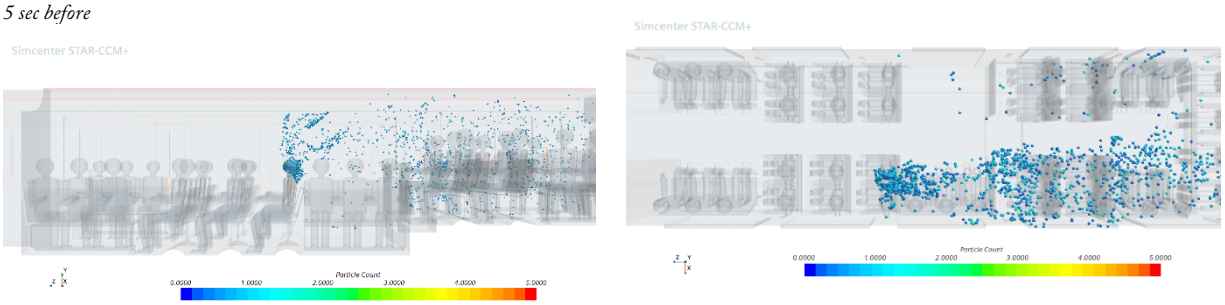

Door Open

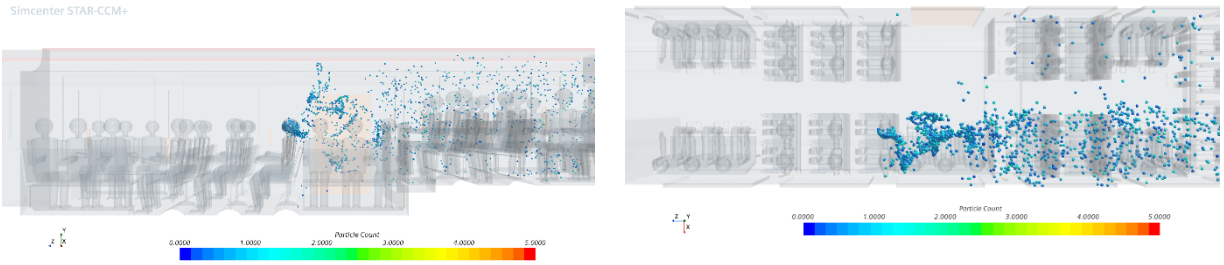

5 sec after Door Open

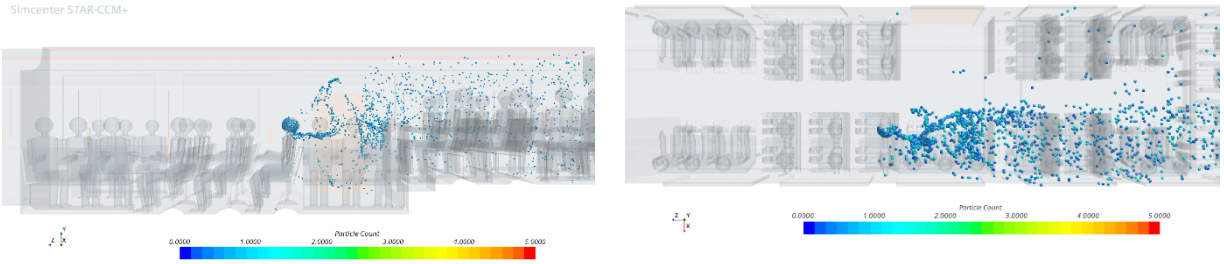

15 sec

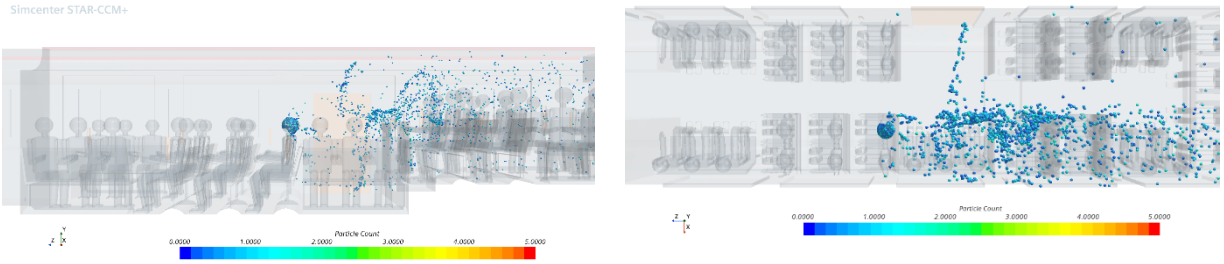

25 sec

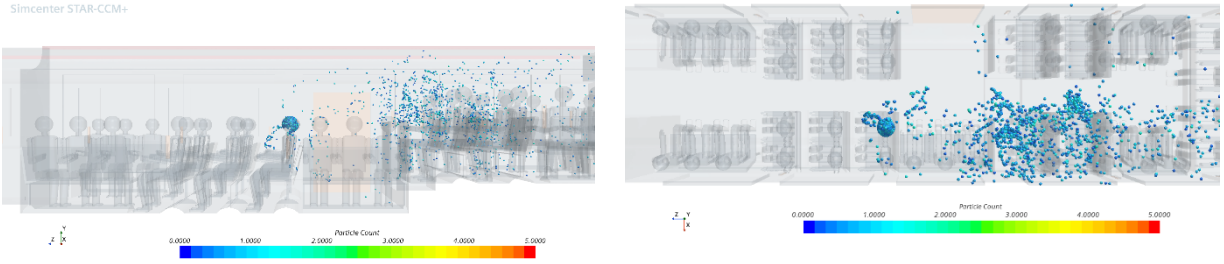

30 sec (Door Closed)

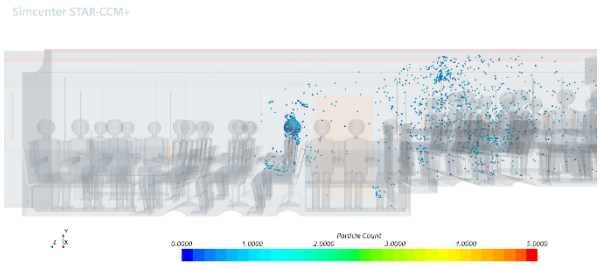

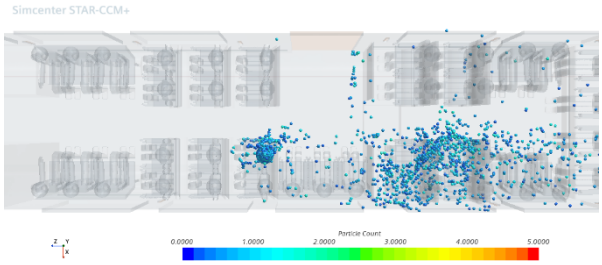

35 sec

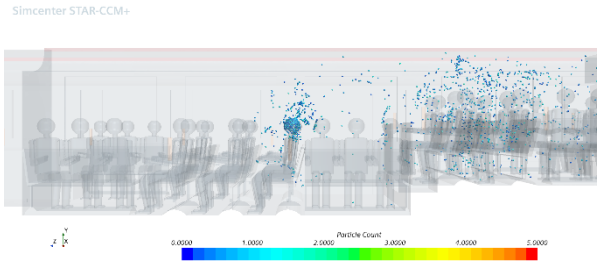

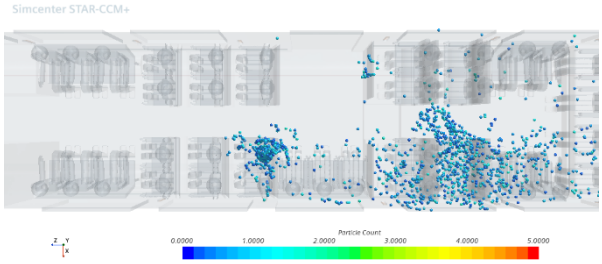

40 sec

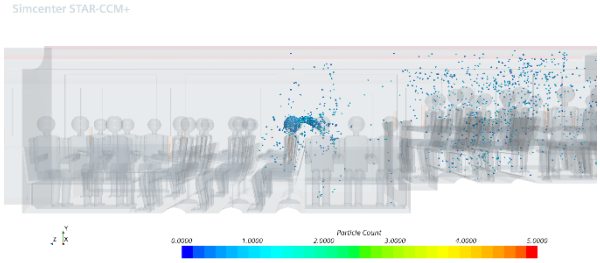

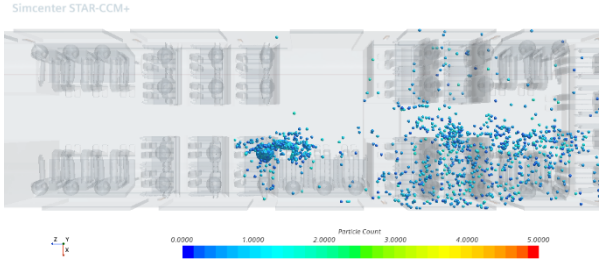

50 sec

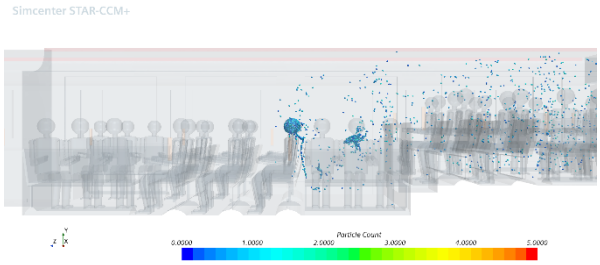

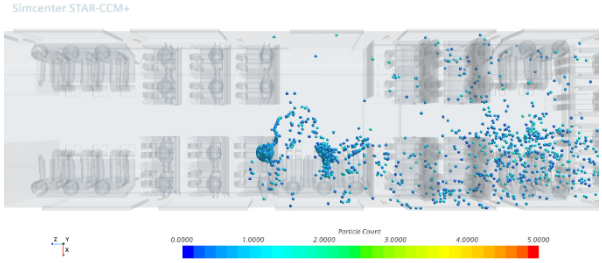

60 sec

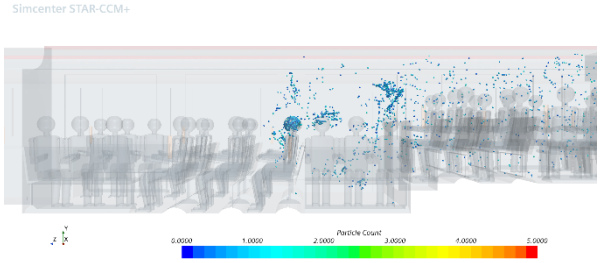

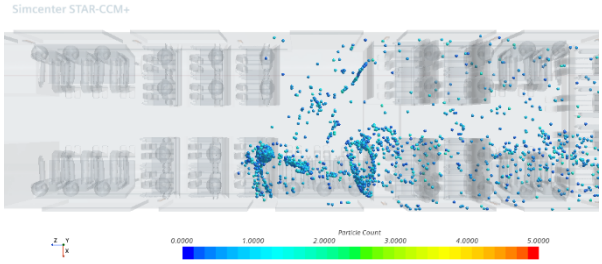

Figure 21. Contours of Axial Vorticity in Open-Closed Door Conditions

Door open Vorticity

5 sec before

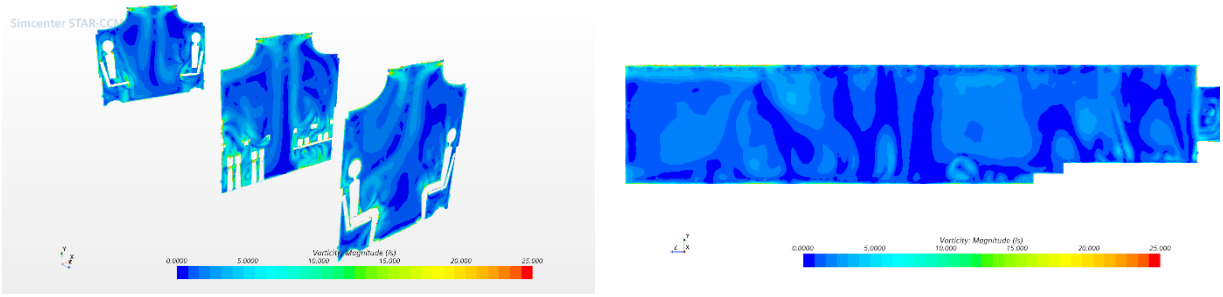

Door Open

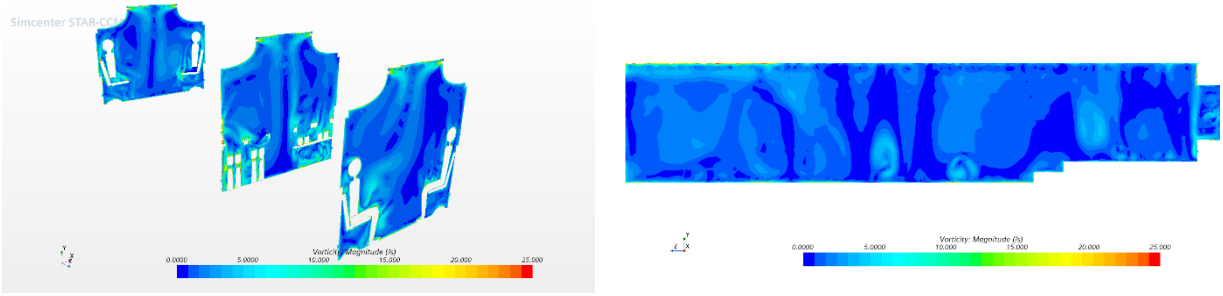

5 sec after Door Open

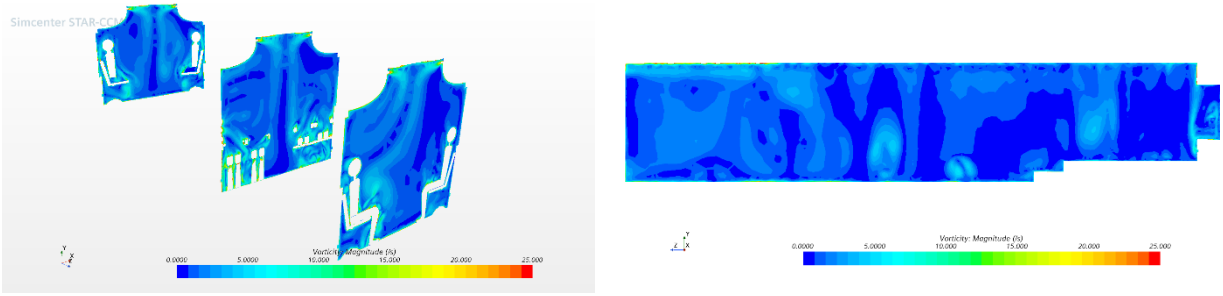

15 sec

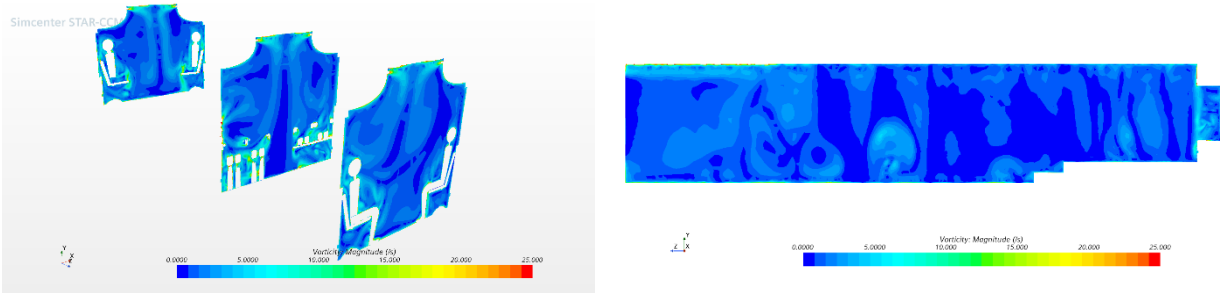

25 sec

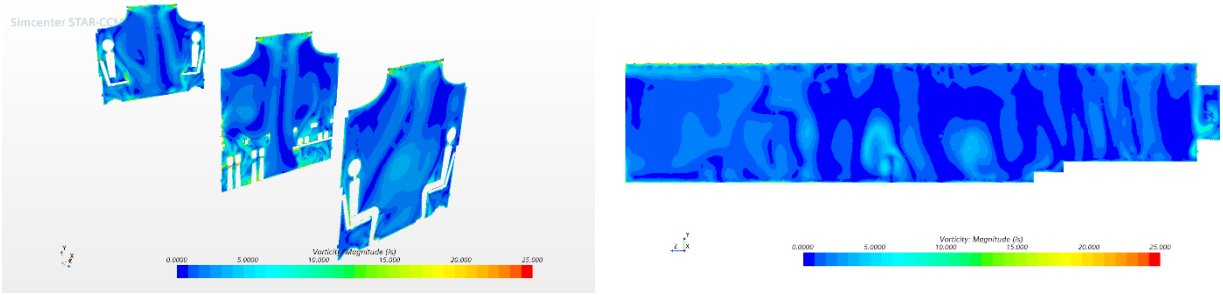

30 sec (Door Closed)

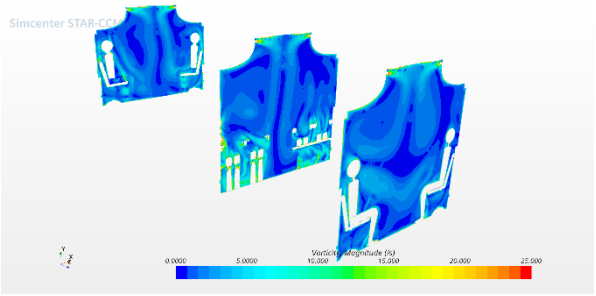

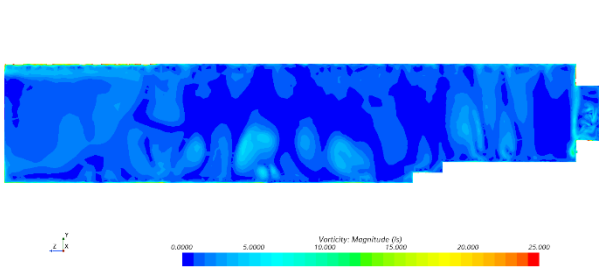

35 sec

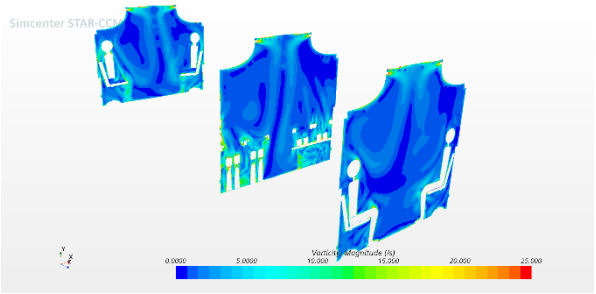

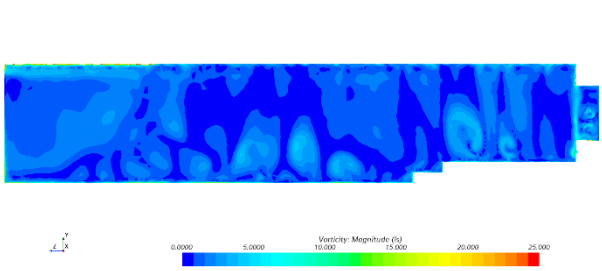

40 sec

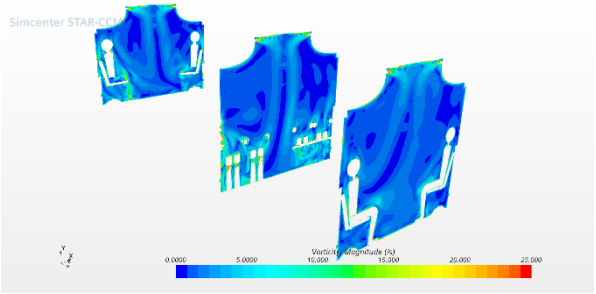

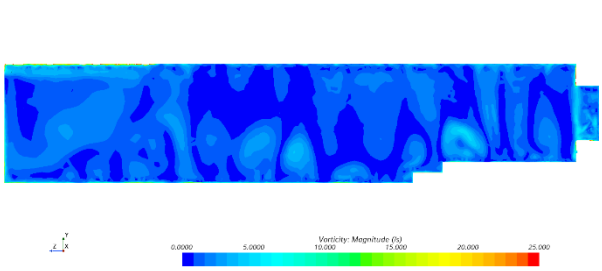

50 sec

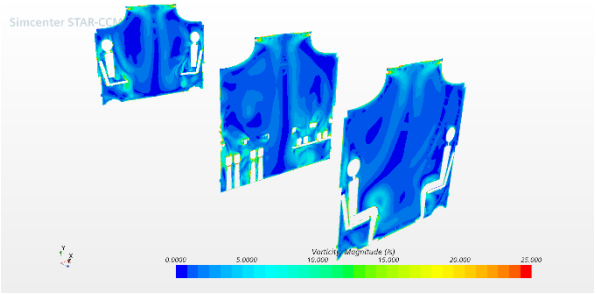

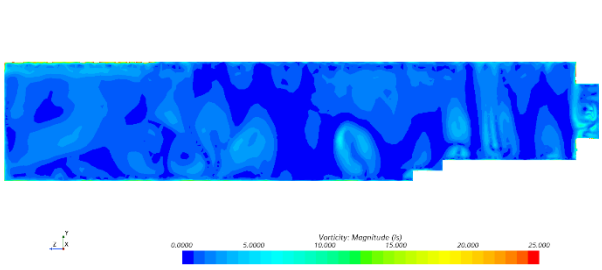

60 sec

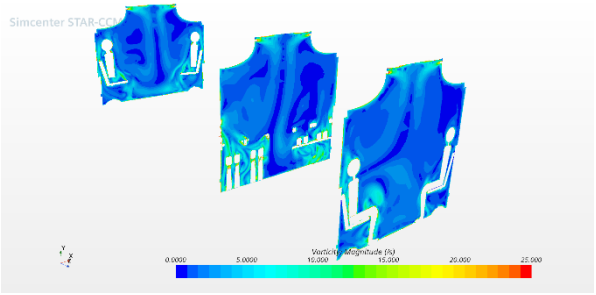

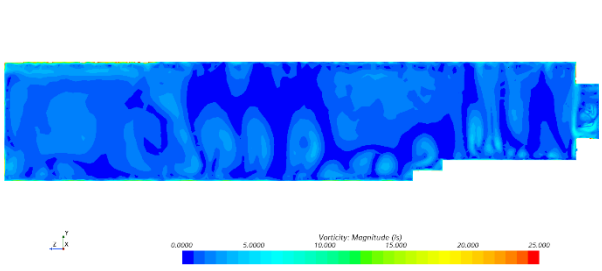

Figure 22. Contours of TKE in Open-Closed Door Conditions

Door open TKE

5 sec before

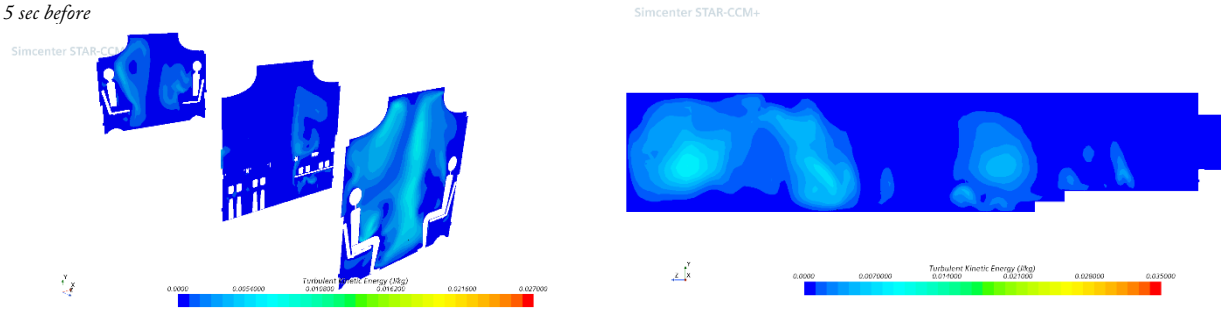

Door Open

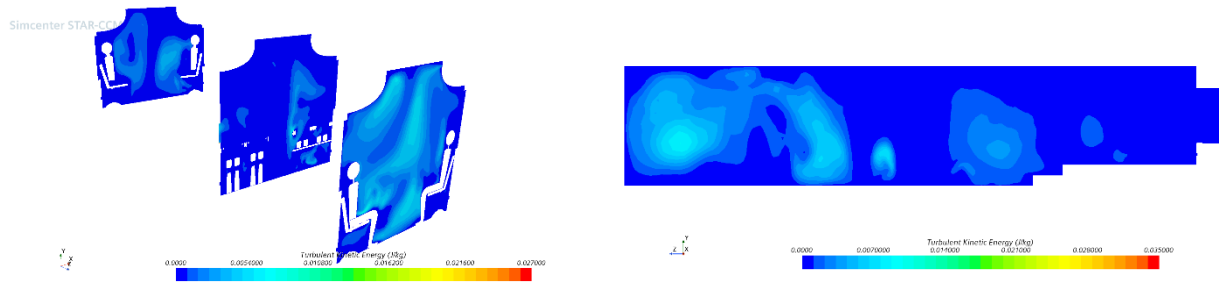

5 sec after Door Open

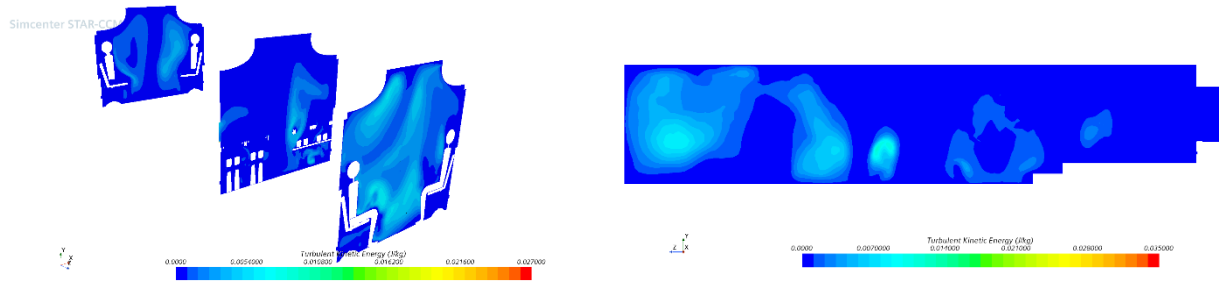

15 sec

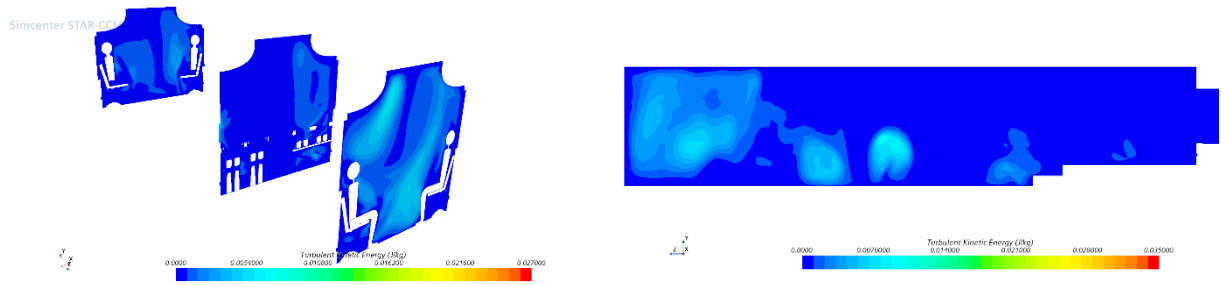

25 sec

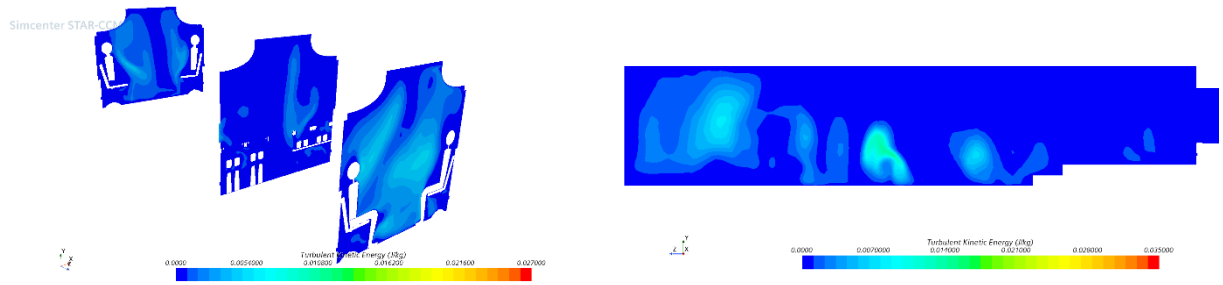

30 sec (Door Closed)

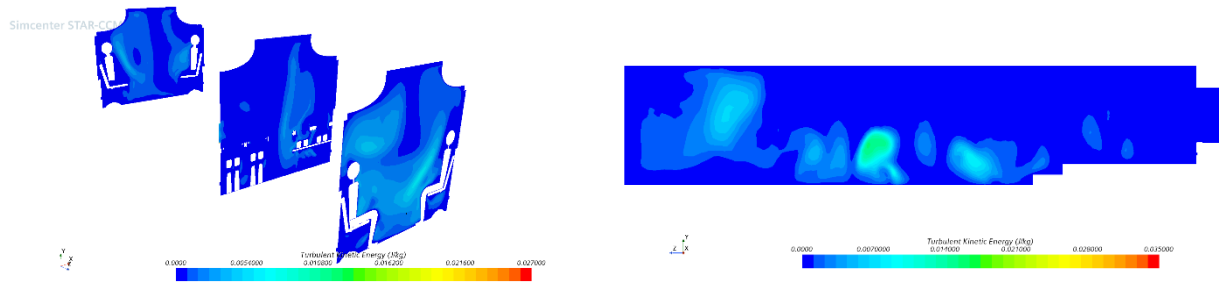

35 sec

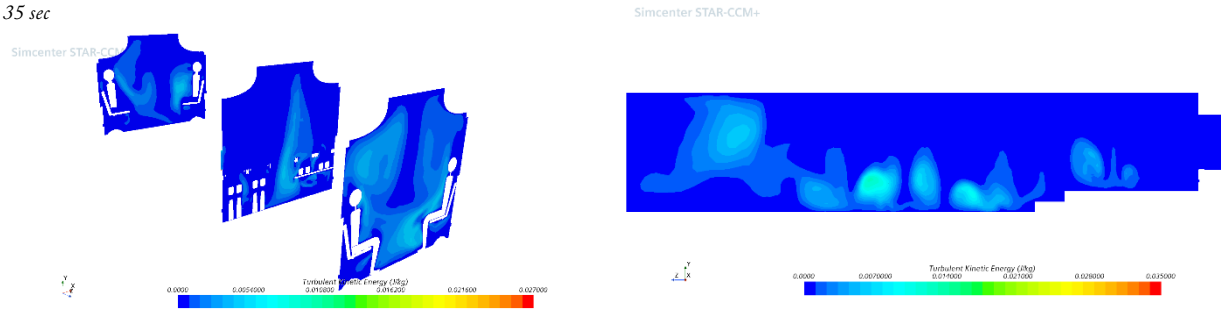

40 sec

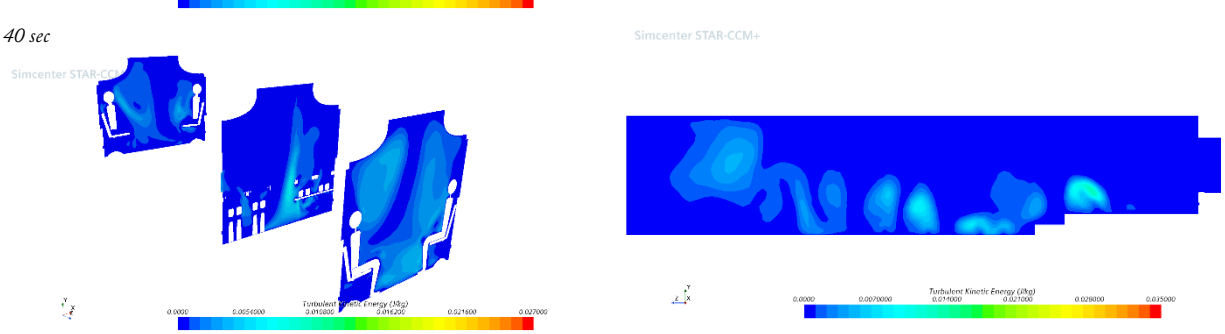

50 sec

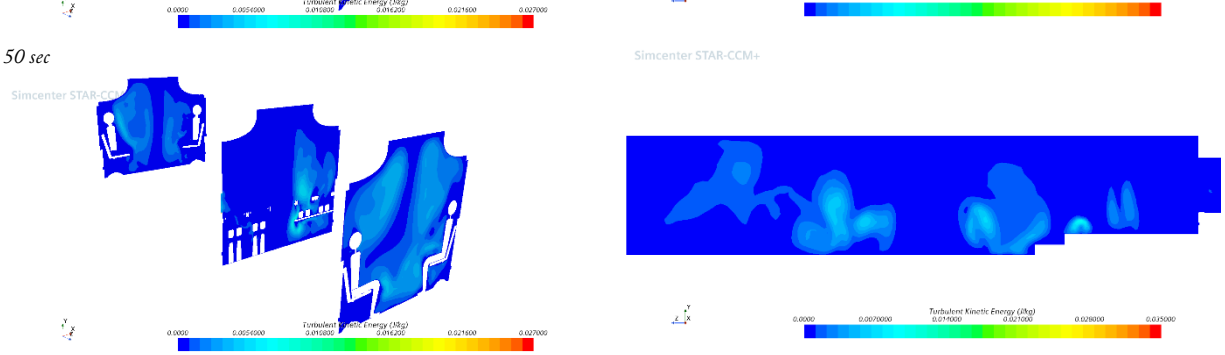

60 sec

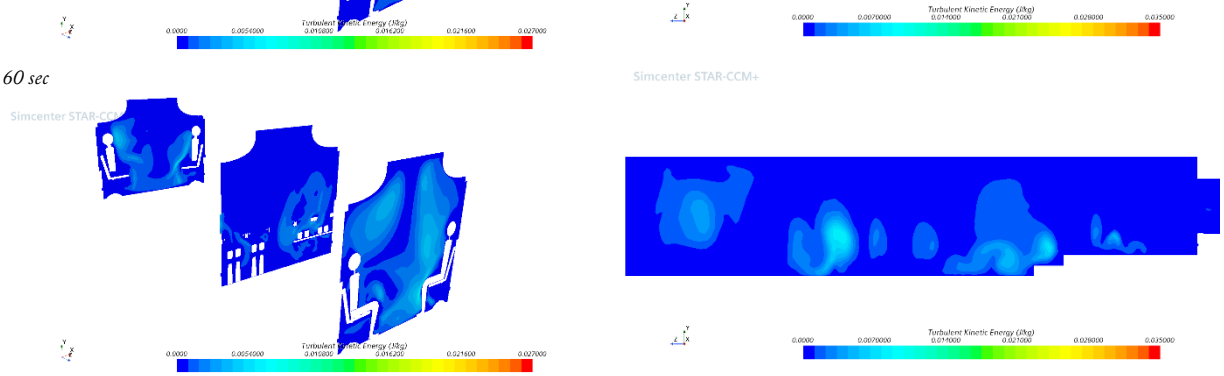

3.3 Analytical Solutions

The Wells-Riley (WR) equation was used to estimate the risk of infection for different riding durations and scenarios. The equation assumes well-mixed air inside the cabin which is not true as evident from our simulations. However, it provides an estimate of the probability of infection with a relatively high level of accuracy. The equation is:

$$\frac{n}{N_s} = \left(1 - e^{\frac{n_0 q_n Q_B t}{Q_T}}\right)$$

Where:

- n is the number of infectious cases
- N_s is the population (in our case 37)
- n_0 is the number of infectors (1 for our case)
- q_n is the quanta generation rate= q_g/(copies/quanta) (0.645 based on previous analyses)
- q_g is the viruses released per min (1,267 in our case)
- Q_B is the person's CFM (0.3)
- Q_T is the room's CFM
- t is the trip duration in minutes
- Ventilation is OFF

When the ventilation is off, the room CFM is calculated based on the volume of the air inside the bus which is equivalent to 2,749 ft^3 based on the dimensions of the bus used. Then, Q_T (CFM) is 2,749/t.

Figure 1 shows the number of infectious passengers with time for three cases of no ventilation, 50% recirculating air and 50% fresh air, and 100% fresh air. In the case of no ventilation, the number of infectious passengers increases very quickly beyond 30 minutes. At 30 minutes, two passengers are infected. The number of passengers increases to eight after 60 minutes and to 23 after 120 minutes. However, with both 50% and 100% fresh air, the infectious rate decreases significantly. At 30 minutes, the risk of infection for these cases reaches, respectively, 0.2 and 0.1 passengers, and at 60 minutes, are 0.4 and 0.2, respectively.

As we have indicated before, the assumption of a fully mixed flow is not valid, and thus with increased virus concentration around the infectious passenger, the risk of infection increases. In the case of the axial slots, the total length of the slots on both sides is approximately 24 m where about 1/12 of that or 2 m of the slot is adjacent to the infectious passenger. For 100% fresh air, the volumetric airflow is 2,097 CFM, and 1/12 of that is approximately 175 CFM. This is the volume of the air movement around the passengers sitting close to the infectious passenger. Assuming 1,267 viruses are released per minute, the virus concentration in this area is 7.24/ft^3.

Virus infectivity and replication is often quantified through the use of 50% tissue culture infectious dose ($TCID_{50}$) assays. A study [18] on the human infectious dose of the Influenza A virus found $TCID_{50}$ = 3 which corresponds to approximately 703±422 viral particles for a one-hour exposure [19]. For our simulation, for one-hour exposure, the total virus/ft^3 is about 434, which is within the range of the human infectious dose, and thus presents a risk for infection.

Figure 23. Analytical Results for the Rate of Infection with Time

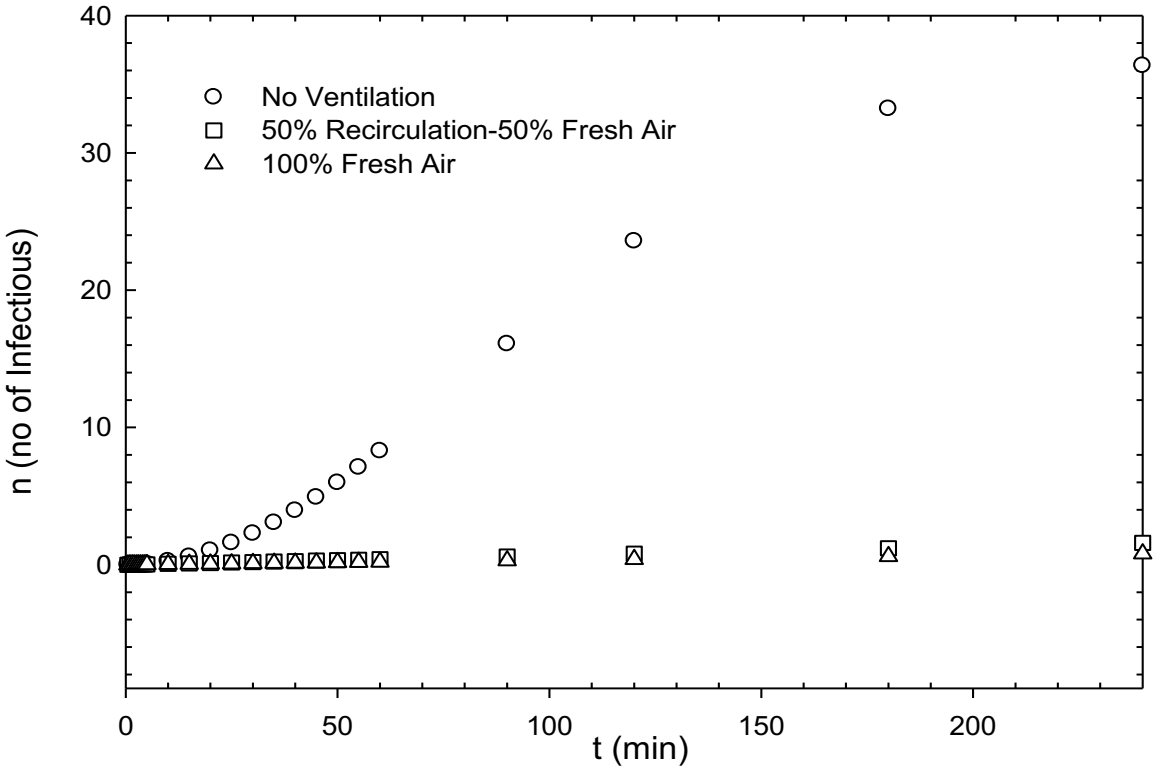

4. Conclusions

Unsteady incompressible Reynolds-Averaged Navier-Stokes (U-RANS) simulations with an SST-kω turbulence model were performed to investigate virus transport released from an infectious passenger aboard a transit bus. The infectious passenger was sitting in the middle of the bus in an aisle seat, releasing 1,267 of 2.5 micron round particles per minute at a mouth velocity of 0.278 m/s (0.3 CFM). Fresh air at a rate of 59.38 m^3/min (2,097 CFM) was injected into the bus through the ceiling liner slots at a velocity of 1 m/s. Two different linear axial and vertical exhausts placed on the side walls were investigated for virus containment. Results show that in both cases, the particles' concentration is limited to around the infectious passenger. With the opening of the passenger's drop-off door and additional air change, the particles spread to the front and back of the bus, but stay on the same side of the bus as the infectious passenger and particles' concentration is reduced. The study shows that increased ventilation and local air control reduce the risk of infection significantly.

The current simulations are for 100% fresh air entering the bus through the ceiling slots and exiting through either the horizontal or vertical slots. In most cases, the bus uses either partial or fully recirculating air to save energy and thus increases the probability of infection. As indicated in the analytical study, the chance of infection increases significantly with a fully-recirculating air but reduces when equal parts of fresh and recirculating air are used. The flexibility of controlling the percentage of fresh air introduced into the bus's ventilation system allows the bus operator and the transit agency to maintain a healthy cabin environment during the flu season and when an increased risk of infection or environmental contamination exists due to an emergency condition.

Endnotes

1. World Health Organization. "Global research on coronavirus disease (COVID-19)." https://www.who.int/emergencies/diseases/novel-coronavirus-2019/global-research-on-novel-coronavirus-2019-ncov (last updated 2023).

2. Nikitin, N., Ekaterina, P., Trifonova, E., and Karpova, O. "Influenza Virus Aerosols in the Air and Their Infectiousness." *Adv. In Virology* vol. 2014, Art IN 859090 (2014).

3. Loudon, R.G., and Roberts, R.M. "Droplet expulsion from the respiratory tract." *The American Review of Respiratory Disease* vol. 95, no. 3 (1967): 435–442.

4. Jennison, M.W. "Atomizing of mouth and nose secretions into the air as revealed by high-speed photography." In *Aerobiology*, F. R. Moulton (ed.) (1942): 106–128, American Association for the Advancement of Science, Washington, DC, USA.

5. Papineni, R.S., and Rosenthal, F.S. "The size distribution of droplets in the exhaled breath of healthy human subjects." *Journal of Aerosol Medicine: Deposition, Clearance, and Effects in the Lung* vol. 10, no. 2 (1997): 105–116.

6. Chao, C.Y.H., Wan, M.P., Morawska, L., et al. "Characterization of expiration air jets and droplet size distributions immediately at the mouth opening." *Journal of Aerosol Science* vol. 40, no. 2 (2009): 122–133.

7. Noti, J.D., Lindsley, W.G., Blachere, F.M., et al. "Detection of infectious influenza virus in cough aerosols generated in a simulated patient examination room." *Clinical Infectious Diseases* vol. 54, no. 11 (2012): 1569–1577.

8. Cowling, B.J., Ip, D.K., Fang, V.J., et al. "Aerosol transmission is an important mode of influenza A virus spread." *Nature Communications* vol. 4, article 1935 (2013).

9. Fabian, P., McDevitt, J.J., DeHaan, W.H., et al. "Influenza virus in human exhaled breath: an observational study." *PLoS ONE* vol. 3, no. 7, Article ID e2691 (2008).

10. Lowen, A.C., Mubareka, S., Tumpey, T.M., Garc´ıa-Sastre, A., and Palese, P. "The guinea pig as a transmission model for human influenza viruses." *Proceedings of the National Academy of Sciences of the United States of America* vol. 103, no. 26 (2006): 9988–9992.

11. Lowen, A.C., Mubareka, S., Steel, J., and Palese, P. "Influenza virus transmission is dependent on relative humidity and temperature." *PLoS Pathogens* vol. 3, no. 10 (2007): 1470–1476.

12. Steel, J., Palese, P., and Lowen, A.C. "Transmission of a 2009 pandemic influenza virus shows a sensitivity to temperature and humidity similar to that of an H3N2 seasonal strain." *Journal of Virology* vol. 85, no.3 (2011): 1400–1402.

13. Leung, N.H.L., et al. Respiratory virus shedding in exhaled breath and efficacy of face masks. Nat Med. 2020 May;26(5):676-680. doi: 10.1038/s41591-020-0843-2. Epub 2020 Apr 3. Erratum in: Nat Med. 2020 May 27;: PMID: 32371934; PMCID: PMC8238571.

14. Taherian, S., Rahai, H.R., Bonifacio, J, and Horstman, R. "Virus Transport Aboard Commercial Regional Jets." *The 44th AIAA Fluid Dynamics Conference*, AIAA Aviation and Aeronautics Forum and Exposition, Atlanta, GA (2014).

15. Horstman, R., and Rahai, H. "A risk assessment of an airborne disease inside the cabin of a passenger airplane." *SAE Int J Advances& Curr Prac in Mobility* 3(3) (2021): 1263–1271. doi:10.4271/2021-01-0036

16. Evaluating vacant middle seats and masks as Coronavirus exposure reduction strategies in aircraft cabins using particle tracer experiments and computational fluid dynamics simulations - Bennett - Engineering Reports - Wiley Online Library

17. Rahai, H., and Bonifacio, J. "Numerical Investigations of Virus Transport Aboard a Commuter Bus." *Mineta Transportation Institute* (MTI) Report No 21-07 (2021).

18. Alford, R.H., Kasel, A., Gerone, P.J., and Knight, V. "Human Influenza Resulting from Aerosol Inhalation." P*roceedings of the Society of Experimental Biology and Medicine* vol. 122, no. 3 (1966): 800–804.

19. Yang, W., Elankumaran, S., and Marr, L.C. "Concentrations and Size Distributions of Airborne Influenza A Viruses Measured Indoor at a Health Center, a Day-Care Center, and on Aeroplanes." *Journal of the Royal Society Interface* vol. 8, no.61 (2011): 1176-1184.

Bibliography

Alford, R.H., Kasel, A., Gerone, P.J., and Knight, V. "Human Influenza Resulting from Aerosol Inhalation." *Proceedings of the Society of Experimental Biology and Medicine* vol. 122, no. 3 (1966): 800–804.

Chao, C.Y.H., Wan, M.P., Morawska, L., et al. "Characterization of expiration air jets and droplet size distributions immediately at the mouth opening." *Journal of Aerosol Science* vol. 40, no. 2 (2009): 122–133.

Cowling, B.J., Ip, D.K., Fang, V.J., et al. "Aerosol transmission is an important mode of influenza A virus spread." *Nature Communications* vol. 4, article 1935 (2013).

Evaluating vacant middle seats and masks as Coronavirus exposure reduction strategies in aircraft cabins using particle tracer experiments and computational fluid dynamics simulations - Bennett - Engineering Reports – Wiley Online Library.

Fabian, P., McDevitt, J.J., DeHaan, W.H., et al. "Influenza virus in human exhaled breath: an observational study." *PLoS ONE* vol. 3, no. 7, Article ID e2691 (2008).

Leung, N.H.L., et al. Respiratory virus shedding in exhaled breath and efficacy of face masks. Nat Med. 2020 May;26(5):676-680. doi: 10.1038/s41591-020-0843-2. Epub 2020 Apr 3. Erratum in: Nat Med. 2020 May 27;: PMID: 32371934; PMCID: PMC8238571.

Loudon, R.G., and Roberts, R.M. "Droplet expulsion from the respiratory tract." *The American Review of Respiratory Disease* vol. 95, no. 3 (1967): 435–442.

Lowen, A.C., Mubareka, S., Tumpey, T.M., Garc´ıa-Sastre, A., and Palese, P. "The guinea pig as a transmission model for human influenza viruses." *Proceedings of the National Academy of Sciences of the United States of America* vol. 103, no. 26 (2006): 9988–9992.

Lowen, A.C., Mubareka, S., Steel, J., and Palese, P. "Influenza virus transmission is dependent on relative humidity and temperature." *PLoS Pathogens* vol. 3, no. 10 (2007): 1470–1476.

Horstman R, and Rahai H. "A risk assessment of an airborne disease inside the cabin of a passenger airplane." *SAE Int J Advances& Curr Prac in Mobility* 3(3) (2021): 1263-1271. doi:10.4271/2021-01-0036.

Jennison, M.W. "Atomizing of mouth and nose secretions into the air as revealed by high-speed photography." In *Aerobiology*, F. R. Moulton (ed.) (1942): 106–128, American Association for the Advancement of Science, Washington, DC, USA.

Nikitin, N., Ekaterina, P., Trifonova, E., and Karpova, O. "Influenza Virus Aerosols in the Air and Their Infectiousness." *Adv. In Virology* vol. 2014, Art IN 859090 (2014).

Noti, J.D., Lindsley, W.G., Blachere, F.M., et al. "Detection of infectious influenza virus in cough aerosols generated in a simulated patient examination room." *Clinical Infectious Diseases* vol. 54, no. 11 (2012): 1569–1577.

Papineni, R.S., and Rosenthal, F.S. "The size distribution of droplets in the exhaled breath of healthy human subjects." *Journal of Aerosol Medicine: Deposition, Clearance, and Effects in the Lung* vol. 10, no. 2 (1997): 105–116.

Rahai, H., and Bonifacio, J. "Numerical Investigations of Virus Transport Aboard a Commuter Bus." *Mineta Transportation Institute* (MTI) Report No 21-07 (2021). 2048-Rahai-Virus-Transport-Bus-Simulations.pdf (sjsu.edu)

Leung, Nancy HL et al, "Respiratory Virus Shedding in Exhaled Breath and Efficacy of Face Mask," Nat. Med. May 2020, 26(5): 676-680. Doi: 10.1038/s41591-020-0843-2

Steel, J., Palese, P., and Lowen, A.C. "Transmission of a 2009 pandemic influenza virus shows a sensitivity to temperature and humidity similar to that of an H3N2 seasonal strain." *Journal of Virology* vol. 85, no.3 (2011): 1400–1402.

Taherian, S., Rahai, H.R., Bonifacio, J, and Horstman, R. "Virus Transport Aboard Commercial Regional Jets." *The 44th AIAA Fluid Dynamics Conference*, AIAA Aviation and Aeronautics Forum and Exposition, Atlanta, GA (2014).

World Health Organization. "Global research on coronavirus disease (COVID-19)." https://www.who.int/emergencies/diseases/novel-coronavirus-2019/global-research-on-novel-coronavirus-2019-ncov (last updated 2023).

Yang, W., Elankumaran, S., and Marr, L.C. "Concentrations and Size Distributions of Airborne Influenza A Viruses Measured Indoor at a Health Center, a Day-Care Center, and on Aeroplanes." *Journal of the Royal Society Interface* vol. 8, no. 61 (2011): 1176–1184.

About the Authors

Hamid Rahai, PhD

Dr. Hamid Rahai is a professor in the Department of Mechanical and Aerospace Engineering & Biomedical Engineering and Associate Dean for Research and Graduate Studies in the College of Engineering at California State University, Long Beach (CSULB). He has taught various classes at the undergraduate and graduate levels in thermal sciences; supervised over 70 M.S. theses, projects, and PhD dissertations; and published more than 90 technical papers. He has received over $13 million in grants and contracts from the National Science Foundation, Federal Highway Administration, California Energy Commission, California Air Resources Board, Port of Los Angeles, Caltrans, Boeing Company, and Southern California Edison, among others. He is the Engineering coordinator for the Caltrans new Local Technical Assistant Program (LTAP) and the director of the Center for Energy and Environmental Research and Services (CEERS) in the College of Engineering at CSULB which includes the Sustainable Engineering Training Academy (SETA) of the LTAP. He has been granted patents for the development of a high-efficiency vertical axis wind turbine (VAWT) and wind turbine apparatuses, and for reducing NOx emission of Cargo Handling Equipment using a Humid Air System. He also has pending patents related to a new conformal vortex generator tape for reducing tip vortices, an environmental artificial tree for reducing ambient NOx, and a new guide-vane enclosure for capturing wind energy from passing vehicles. Dr. Rahai is the recipient of the 2004 Northrop Grumman Excellence in Teaching Award and the 2012 CSULB Impact Accomplishment of the Year in RSCA Award. He received the Outstanding Engineering Educator Award from the Orange County Engineering Council in California in 2014, and in 2019 he was inducted as a senior member of the National Academy of Inventors (NAI).

Jeremy Bonifacio, PhD

Dr. Jeremy Bonifacio is a teaching professor and a senior researcher at the Center for Energy and Environmental Research and Services (CEERS) in the College of Engineering at California State University, Long Beach (CSULB). His expertise is in experimental and computational fluid mechanics. He has been involved in various applied industrial projects at CEERS and is co-owner of several patents related to emission control technologies and the application of CFD in diagnosing lung diseases. Dr. Bonifacio is the winner of the CSULB 2014 innovation challenge.

MTI FOUNDER

Hon. Norman Y. Mineta

MTI BOARD OF TRUSTEES

Directors